

## Article

# Evaluation of Groundwater Vulnerability in the Upper Kelkit Valley (Northeastern Turkey) Using DRASTIC and AHP-DRASTICLu Models

Ümit Yıldırım 

Department of Interior Architecture and Environmental Designing, Faculty of Arts and Designing, Bâberti Campus, Bayburt University, 69000 Bayburt, Turkey; umit.yildirim.1907@gmail.com

**Abstract:** This study aimed to investigate groundwater vulnerability to pollution in the Upper Kelkit Valley (NE Turkey). For this purpose, vulnerability index maps were created using the generic DRASTIC and AHP-DRASTICLu models. The latter model was suggested by adding a parameter to the DRASTIC model and weighting its parameters with the analytical hierarchy process with the GIS technique. The results showed that areas with high and very high vulnerabilities are concentrated around the Kelkit Stream, which flows from east to west in the central part of the study area. In contrast, areas with low and very low vulnerability classes are located in the northern and southern parts of the study area. To validate the model results, a physicochemical characterization of groundwater samples and their corresponding vulnerability index values were statistically compared using the Spearman correlation method. In addition, the single-parameter sensitivity method was applied to analyze the models' sensitivities. Results revealed a stronger correlation between the vulnerability index values of the AHP-DRASTICLu model (compared to the DRASTIC model) in terms of sulfate ( $R^2 = 0.75$ ) and chloride ( $R^2 = 0.76$ ), while there was a slightly weaker correlation for the electrical conductivity ( $R^2 = 0.65$ ) values of the groundwater samples. Sensitivity analysis indicated that the vadose zone, aquifer media, and land use are the most influential parameters responsible for the highest variation in the vulnerability index. Generally speaking, the results indicated that the AHP-DRASTICLu model performs better than the DRASTIC model for investigating groundwater vulnerability to pollution in the Upper Kelkit Valley.



**Citation:** Yıldırım, Ü. Evaluation of Groundwater Vulnerability in the Upper Kelkit Valley (Northeastern Turkey) Using DRASTIC and AHP-DRASTICLu Models. *ISPRS Int. J. Geo-Inf.* **2023**, *12*, 251. <https://doi.org/10.3390/ijgi12060251>

Academic Editors: Wolfgang Kainz and Godwin Yeboah

Received: 5 March 2023

Revised: 15 May 2023

Accepted: 19 May 2023

Published: 19 June 2023



**Copyright:** © 2023 by the author. Licensee MDPI, Basel, Switzerland. This article is an open access article distributed under the terms and conditions of the Creative Commons Attribution (CC BY) license (<https://creativecommons.org/licenses/by/4.0/>).

## 1. Introduction

The ever-increasing population on a global scale has resulted in an increase in needs and therefore an increase in the resulting waste. This situation creates significant pressure on the environment, and this pressure is increasing day by day. In addition, climate change, in which the increasing population also has a large share, puts tremendous pressure on the environment [1]. This pressure mainly affects water resources [2]. Climate change projections reveal that the precipitation that Turkey receives in the future will decrease, leading to a decrease in water resources and, thus, the amount of usable water [3]. Model projections based on the IPCC—A2 pessimistic scenario show that there will be a 16% and 27% reduction in water potentials in Turkey by 2050 and 2075, respectively. This decrease in water potential due to the pressure of climate change [4] reveals the importance of using the existing water resources more effectively. In addition, keeping the quality of available water resources at a functional level is essential for this case.

Freshwater resources for human systems and ecosystems consist of groundwater and surface water resources. Groundwater supplies approximately half of the world's drinking water resources [5] and about 43% of all the water effectively used for irrigation [6]. Groundwater has a lower pollution potential compared to surface water, but polluted

groundwater takes a longer to clean up [7]. Especially in the ever-increasing agricultural activities, the water leaking into the ground due to fertilizers and pesticides used for product development and protection also reduces groundwater quality [8,9]. In addition, anthropogenic wastes in areas where industry and urbanization are intense and also decrease groundwater quality [10].

One of the universal human rights is access to safe fresh water [11]. In addition, an extended access to safe drinking water and sanitation is mentioned in the Sustainable Development Goals [12]. Sustainable freshwater management has gained a significant importance both on a regional [13] and global scale [14–16] and, thus, “Integrated Water Resources Management” has become a scientific paradigm. Groundwater vulnerability assessments can be integrated into Integrated Water Resources Management with tiered approaches to assess vulnerability, hazard potential, and risk.

Margat began studies on groundwater vulnerability to surface pollutants in the 1960s in France [17]. However, this kind of study did not gain popularity until the 1990s due to applicability restrictions. In parallel with the advancements in computer systems in the 1990s, with the development of remote sensing/GIS software, new methodologies began to emerge in groundwater vulnerability studies and started to be applied in various regions of the world [18–20]. Among these methods, the most popular of the overlay-and-index-based methods are SINTACS [21], AVI [19], GOD [22], and DRASTIC [23] applied to porous aquifers and EPIK [24], PI [25], and COP [26] models applied to karstic aquifers. All these methods can be performed within a GIS-based framework where they are used to identify areas more vulnerable to pollution than others or to select the most suitable areas for well sites and/or hazardous land use activities. The most widely used method worldwide among all the overlay-and-index-based methods is the DRASTIC method [27–30], which combines seven hydrogeological parameters (D: depth of water table; R: net recharge; A: aquifer media; S: soil media; T: topography; I: impact of the vadose zone; C: hydraulic conductivity) that are thought to affect the vulnerability of all regions.

In recent years, the number of multidimensional evaluation studies on groundwater vulnerability to pollution has increased. Many researchers suggested changes in the algorithms to develop the generic DRASTIC model, and new DRASTIC-based models were introduced [31–39]. Many studies have been published using the analytical hierarchy process (AHP) [40,41], fuzzy analytical hierarchy process (FAHP) [42,43], evidential belief function (EBF) [44], and logistic regression (LR) [45]. All these methods have been applied to adjust the rate and weight of the criteria and subcriteria in the DRASTIC-based models depending on local hydrogeological conditions.

The analytical hierarchy process method, the most widely used method among the Multicriteria decision making (MCDM) methods, provides excellent convenience in determining the weight values of the criteria on the groundwater vulnerability of the models by pairwise comparisons depending on the hydrogeoenvironmental conditions of the study area. When the AHP method is integrated into the Geographic Information System, it becomes a tool for decision makers to develop sustainable environmental policies as an efficient machine learning technology.

In this study, the impact of standard weights and rates and AHP-based optimized weights and rates on the development of groundwater vulnerability mapping was compared and analyzed using generic DRASTIC and AHP-DRASTICLu models for the Upper Kelkit Valley (North Turkey). The data obtained in both models were compared statistically with the physicochemical content of the groundwater samples taken from the study area, and the statistically related parameters were determined along with which model was more correlated with the observed groundwater physicochemical analysis results. The Upper Kelkit Valley has a semi-arid climate in the northeast of Turkey. Compared to other large basins in Turkey, it is a region prone to water scarcity [3]. Regarding land use classes, more than half of the study area is of the farming activity class. The livelihoods of the majority of the local people depend on farming activity. Considering the population growth, an increase in the amount of agricultural activities, and therefore also in the chemical fertilizers

used for product development, will be inevitable. Such activities on the land surface can disrupt essential natural ecosystem functions [46] and pose a threat to human health through a variety of exposure pathways [47]. In addition, groundwater is also used as drinking water in some parts of the study area. Therefore, studies on groundwater pollution in the Upper Kelkit Valley are a necessity for the proper management of groundwater and environmental planning. In addition, there are no studies on groundwater vulnerability in any terms in the region, and this study is a completely new attempt with the DRASTICLu model optimized with the combination of the AHP. Further, this new model, produced by adding land use criteria to the generic DRASTIC model and progressing the rates and weights of all criteria and subcriteria using the AHP, compared to previous models, will provide excellent convenience for groundwater vulnerability assessments in the areas similar to the UKV in terms of hydrogeoenvironmental conditions.

Overall, this study aims to establish a groundwater vulnerability map of the Upper Kelkit Valley and provide proven bases for sustainable water management. In addition, modifying the generic DRASTIC model to create a more accurate groundwater vulnerability assessment model is also one of the aims of this study. Furthermore, this study aims to assess the relative importance of the parameters used in the models through sensitivity analysis for assessing aquifer vulnerability.

## 2. Materials and Methods

### 2.1. Description of the Study Area

The Upper Kelkit Valley (UKV) forms the upper parts of the Kelkit Valley, representing the upper parts of the Yeşilırmak Basin, one of Turkey's 25 largest river basins. The UKV extends between latitudes  $40^{\circ}03'45''$ – $40^{\circ}13'00''$  N and longitudes  $39^{\circ}12'03''$ – $39^{\circ}42'13''$  E and is located on the border of the Gümüşhane and Bayburt provinces (Figure 1). The topographic heights of the UKV, which covers an area of  $445 \text{ km}^2$ , vary between 1357 and 2297 m a.m.s.l. (Figure 2a). In the study area with generally low land slope, the slopes vary between 0 and  $18^{\circ}$  in approximately 60% of its area (Figure 2b, Table 1).

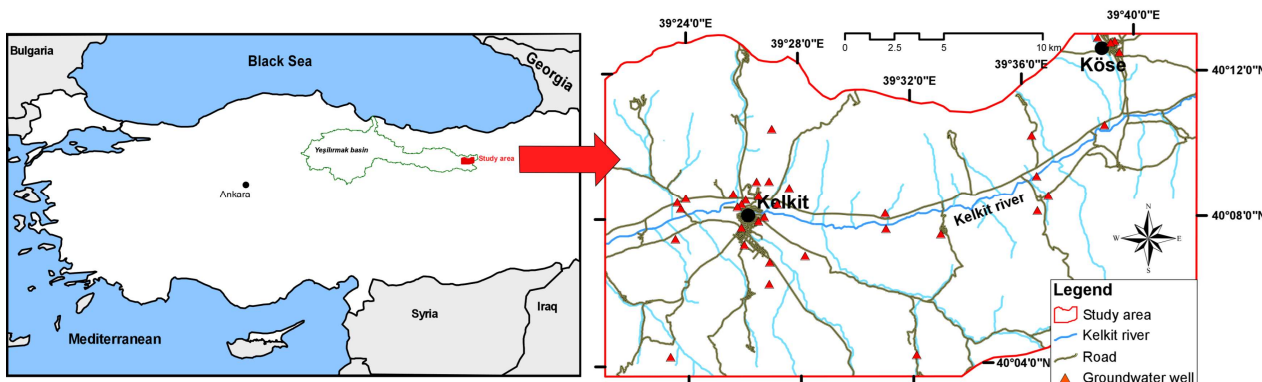


**Figure 1.** The location map of the Upper Kelkit Valley (UKV) includes the location of the wells for use to measure the distance to groundwater.

The study area is located on the border of the Black Sea and the Eastern Anatolia Region and has transitional climatic conditions. Summers are cool; winters are quite cold and rainy. The meteorological measurements between 2003 and 2021 showed that the average annual precipitation in the Kelkit region was 300 mm and the average annual temperature was  $6.5^{\circ}\text{C}$  [48]. The most common soil type in the study area is brown soil covering an area of 77% (Figure 2c, Table 1). The rest consists of brown forest soil, bare rock, colluvium, noncalcareous brown forest soil, alluvium, settlement, and floodplain (Figure 2c).

**Table 1.** Basic characteristics of the Upper Kelkit Valley (UKV).

Characteristics	Unit	Value	Characteristics	Unit	Value
The study area (total)	km <sup>2</sup>	445	<i>Soil type</i>	% area	77.12
<i>Meteorology</i>			Brown soil	% area	5.84
Precipitation (total mean)	mm/year	300	Brown forest soil	% area	5.25
Temperature (mean)	°C	6.5	Bare rock	% area	4.69
<i>Slope range</i>			Colluvium	% area	2.16
0°–2°	% area	6.28	Noncalcic brown forest soil	% area	3.03
2°–6°	% area	18.61	Alluvium	% area	0.96
6°–12°	% area	21.08	Settlement	% area	0.94
12°–18°	% area	15.02	Floodplain	% area	
>18°	% area	39.01	<i>Geology</i>		
<i>Elevation range (a.m.s.l.)</i>			Kelkit Formation	% area	44.01
1357–1500 m	% area	25.03	Berdiga Formation	% area	28.36
1500–1750 m	% area	54.72	Şenköy Formation	% area	15.30
1750–2000	% area	17.62	Alluvium	% area	11.18
2000–2297 m	% area	2.64	Köse Granite	% area	1.15

The UKV can be described as a rural area considering the settled population and land use classes. The UKV includes the Kelkit and Köse districts, which have populations of 44,068 and 7774, respectively [49]. The populations of these districts in 2007 were 41,664 (Kelkit) and 7270 (Köse), and their population growth rates are 12.64% (Kelkit) and 10.9% (Köse) [49]. This population increases even more during the summer seasons with the visits of relatives (i.e., grandparents, parents, siblings, children, and grandchildren) of citizens living in other cities or abroad. Arable land (35.55%) and agricultural lands (17.69%) are the land use classes that cover more than half of the UKV. Arable land, the most common land use type, is located around the Kelkit Stream, the main stream along the northeast–southwest direction of the UKV, in regions with an average slope of 4.5° and elevations between 1360 m and 1914 m. The rest are agricultural areas, open space, natural grassland, pastures, shrub, forest, settlement, water bodies, mines, and dump areas (Figure 3d).

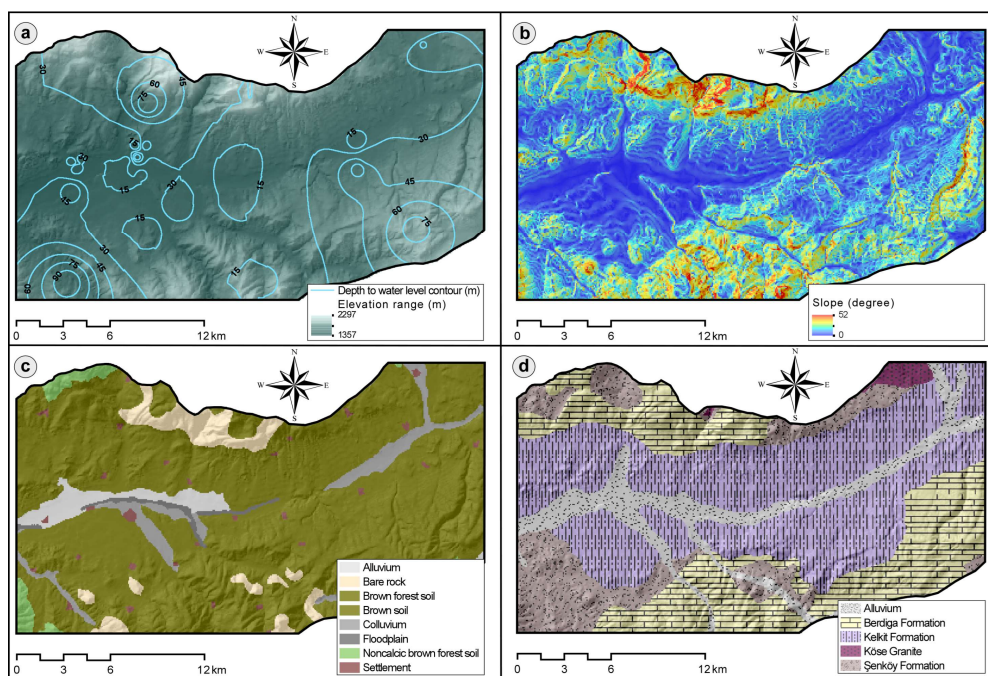


**Figure 2.** Maps showing (a) digital elevation model with the depth to groundwater table contour, (b) slope in degree, (c) soil type [50], and (d) geology—modified from [51].

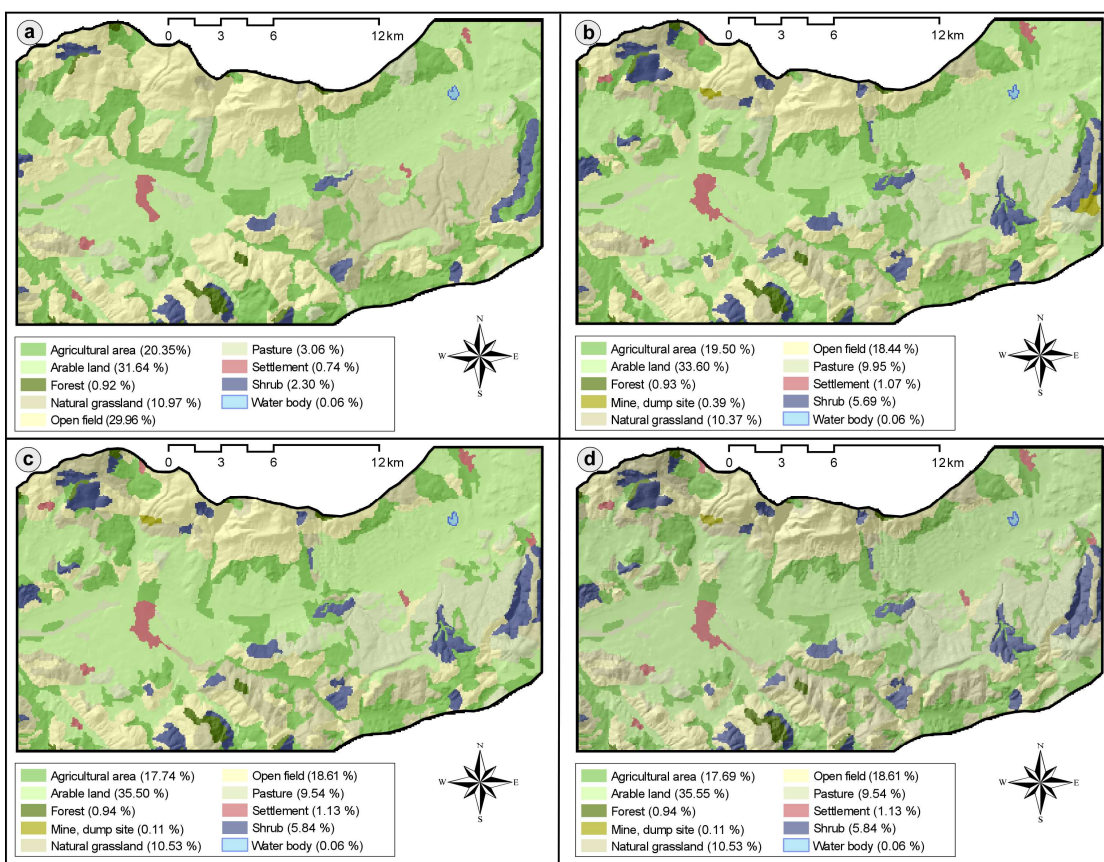


**Figure 3.** Spatial distribution of land use classes and areas covered in 2000 (a), 2006 (b), 2012 (c), and 2018 (d) in the Upper Kelkit Valley [52–55].

Considering the temporal changes of the land use types in the study area [52–55], the 2000–2018 period witnessed a notable decrease in open spaces (29.96% and 18.61%) along with an increase in pastures (3.06% and 9.54%) and arable land (31.64% and 35.55%) (Figure 3, Table 2). The study area's residents mostly live from agriculture and animal husbandry activities. The increase in the agricultural and pasture areas in the study area through time can be explained by the increasing population growth rate and the fact that agriculture and animal husbandry are the main sources of income in the region. Irrigation water needed for the execution of farming activities is provided from the Kelkit Stream and its branches passing through the middle of the study area and from underground water wells. In addition, a large portion of the residents in the study area use the groundwater resources as drinking water.

**Table 2.** Land use classes and areas covered by years in the Upper Kelkit Valley [52–55].

Land Use/Land Classes	2000	2006	2012	2018 *
Agricultural area	20.35	19.50	17.74	17.69
Arable land	31.64	33.60	35.55	35.55
Forest	0.92	0.93	0.94	0.94
Natural grassland	10.97	10.37	10.53	10.53
Open field	29.96	18.44	18.61	18.61
Pasture	3.06	9.95	9.54	9.54
Settlement	0.74	1.07	1.13	1.13
Shrub	2.30	5.69	5.84	5.84
Water body	0.06	0.06	0.06	0.06
Mine and dump site	-	0.39	0.11	0.11

\* Land use classes used for the AHP-DRASTICLu model.

The lithological basement unit in the study area is the Late-Carboniferous-aged Köse Granite [56,57], which is abundantly cracked and partially weathered [58] and crops out around the Köse settlement area in the north of the UKV. The Şenköy Formation spreading in different regions of the north and south of the study area [58], consisting of Liassic volcano sediments [59–61], overlies this unit unconformably. The Şenköy Formation is conformably overlain by the Berdiga Formation [60–64], which is Jurassic-Lower Cretaceous-aged shallow platform carbonates. The Berdiga Formation mainly consists of limestone, dolomite, and dolomitic limestone layers with conglomerate, sandstone, and silt successions that cover large areas in the northern and southern parts of the study area (Figure 2d, Table 1). The Early–Middle-Eocene-aged Kelkit Formation (Figure 2d, Table 1), which outcrops in an east–west direction in the central parts of the study area, unconformably overlies the Şenköy and Berdiga Formations [51,65]. The formation mainly consists of volcanic and volcano-sedimentary rocks with abundantly fractured structures [58]. Alluviums (Figure 2d), which contain fragments of surrounding rocks from clay to coarse pebbles and generally outcrop along the Kelkit Stream, form the quaternary units in the study area [58].

According to the aquifer classification, considering the lithologies of the geologic formations in the UKV, the common aquifer types are the unconsolidated aquifer representing the alluvial material around Kelkit Stream, the semi-consolidated aquifer formed by the units of the Kelkit Formation surrounding this alluvial unit, and the karstic aquifer representing the Berdiga Formation scattered around the semi-consolidated aquifer unit in the northern and southern parts. In the study area, groundwater wells are mainly concentrated on unconsolidated and semi-consolidated aquifers around the Kelkit Stream. Groundwater abstracted from these aquifers and Kelkit Stream water is the primary water source for agricultural and domestic use in the region. The Kelkit Stream, which flows through the study area in the northeast–southwest direction with a perennial annual average discharge rate of  $0.403 \text{ m}^3/\text{s}$  [66], has an approximately 36 km main channel and its tributaries. Near the stream zone, the depth of groundwater is usually less than 1 m, and it rises to 99 m in areas with high altitudes (Figure 2a). Groundwater recharge to the aquifer is chiefly due to precipitation, subsurface inflows from the recharge area and Kelkit Stream channels, and agricultural irrigation.

## 2.2. Vulnerability Assessment Using DRASTIC and AHP-DRASTICLu Models

One of the most common methods used to estimate the vulnerability of aquifers to pollution is the US Environmental Protection Agency's DRASTIC [23] model. Although this model, which is a grid-cell-based overlay and index model, was not GIS-integrated at first, it was later modified by different researchers to various forms with the integration of GIS to further improve its pollution prediction capabilities in different physical environments [31–33,67]. In this study, both the DRASTIC model and the AHP-DRASTICLu model, which is a modified version of the DRASTIC model with the analytic hierarchy process, one of the multicriteria decision-making methods, were applied to the UKV to determine the groundwater vulnerability to pollution.

The DRASTIC method has two primary stages. First, the hydrogeological and geomorphological mappable parameters affecting groundwater pollution are classified. Then, using the determined coefficients, the parameters are weighted, and the vulnerability index is calculated [23].

Each letter of the word DRASTIC represents a hydrogeologically and morphologically mappable parameter [23]. These parameters are listed as follows:

D: Depth to water table, R: Net recharge, A: Aquifer media, S: Soil media, T: Topography, I: Impact of vadose zone, C: Hydraulic conductivity. In the method, each parameter is rated ( $r$ ), and weighted ( $w$ ), and vulnerability maps are created on the GIS platform using the formula shown in Equation (1) determined for DRASTIC vulnerability index ( $DV_i$ ) calculation [23].

In the rating ( $r$ ) stage, each parameter of the DRASTIC model is considered a factor affecting pollution, and values ranging from 1 to 10 are assigned to these factors according

to their relative pollution potential (Tables 3 and 4). “1” represents low potential, and “10” represents high potential. In the weighting (w) stage, weight values ranging from “1” (lowest importance) to “5” (highest importance) are assigned to each parameter that makes up the DRASTIC model, depending on their effects in transporting land-based pollutants to groundwater (Tables 3 and 4).

**Table 3.** The pairwise comparison matrix and normalized weight ( $w_i$ ) of the AHP-DRASTICLu model criteria and weight ( $w_i$ ) of DRASTIC model criteria.

Main Criteria	(D)	(R)	(A)	(S)	(T)	(I)	(C)	(Lu)	AHP-DRASTICLu $w_i$	DRASTIC $w_i$
<b>(D) Depth to water table</b>	1								<b>0.248</b>	5
(R) Net recharge	1/2	1							0.143	4
(A) Aquifer media	1/3	1/2	1						0.081	3
(S) Soil media	1/7	1/3	1/2	1					0.047	2
(T) Topography	1/9	1/6	1/4	1/3	1				0.024	1
(I) Impact of vadose zone	1	2	4	3	7	1			0.237	5
(C) Hydraulic conductivity	1/3	1/3	1/2	2	3	1/4	1		0.065	3
(Lu) Land use classes	1/2	1	3	5	6	1/2	2	1	0.154	

The most important subcriteria and their values are written in bold.

**Table 4.** The pairwise comparison matrix and normalized weight ( $w_i$ ), standardized ratings ( $r_i$ ) and total weight ( $r_i \times w_i$ ) of the subcriteria of AHP-DRASTICLu and DRASTIC models.

Subcriteria	(1)	(2)	(3)	(4)	(5)	(6)	(7)	(8)	(9)	(10)	AHP-DRASTICLu		DRASTIC	
											$r_i$	$w_i$	$r_i \times w_i$	$r_i$
<i>Depth to water table (m)</i>														
(1) 0–1.52											0.352	0.0876	10	50
(2) 1.52–4.57	1/2	1									0.231	0.0573	9	45
(3) 4.57–9.14	1/3	1/2	1								0.157	0.0389	7	35
(4) 9.14–15.24	1/4	1/3	1/2	1							0.112	0.0278	5	25
(5) 15.24–22.86	1/5	1/4	1/3	1/2	1						0.075	0.0186	3	15
(6) 22.86–30.48	1/7	1/5	1/4	1/4	1/2	1					0.051	0.0126	2	10
(7) 30.48<	1/9	1/7	1/7	1/6	1/6	1/5	1				0.022	0.0055	1	5
<i>Net recharge</i>														
(1) Very low	1										0.041	0.0059	1	4
(2) Low	2	1									0.056	0.0081	3	12
(3) Moderate	3	5	1								0.149	0.0213	5	20
(4) High	7	6	2	1							0.276	0.0395	8	32
(5) Very high	9	7	5	2	1						0.478	0.0684	10	40
<i>Aquifer media</i>														
(1) Alluvium	1										0.433	0.0351	8	24
(2) Massive limestone	1/2	1									0.255	0.0208	7	21
(3) Banded sandstone, limestone, and shale	1/3	1/2	1								0.174	0.0141	6	18
(4) Igneous	1/7	1/5	1/4	1							0.046	0.0037	4	12
(5) Weathered metamorphic/igneous	1/5	1/3	1/3	3	1						0.091	0.0074	5	15
<i>Soil media</i>														
(1) Alluvium	1										0.145	0.0068	9	18
(2) Brown soil	1/5	1									0.047	0.0022	5	10
(3) Bare rock	3	5	1								0.263	0.0124	10	20
(4) Floodplain	2	4	1/2	1							0.172	0.047	0.0082	9
(4) Colluvium	1/3	3	1/3	1/4	1						0.079	0.0037	6	12
(5) Brown forest soil	1/5	1/2	1/5	1/5	1/3	1					0.035	0.0016	3	6
(6) Noncalcareous brown forest soil	1/5	1/2	1/5	1/5	1/3	1	1				0.037	0.0017	3	6
(7) Settlement	2	5	1/2	3	5	4	3	1			0.221	0.0104	10	20

**Table 4.** Cont.

Subcriteria	AHP-DRASTICLu										DRASTIC					
	(1)	(2)	(3)	(4)	(5)	(6)	(7)	(8)	(9)	(10)	$r_i$	$w_i$	$r_i \times w_i$	$r_i$	$w_i$	$r_i \times w_i$
<i>Topography (slope %)</i>																
(1) 0–2	1										<b>0.424</b>		0.0102	<b>10</b>		<b>10</b>
(2) 2–6	1/2	1									0.287	0.024	0.0069	9		9
(3) 6–12	1/3	1/2	1								0.162		0.0039	5	1	5
(4) 12–18	1/5	1/5	1/2	1							0.086		0.0022	3		3
(5) 18<	1/5	1/6	1/5	1/3	1						0.042		0.0010	1		1
<i>Impact of vadose zone</i>																
(1) Alluvium	1										<b>0.431</b>		<b>0.1022</b>	8		<b>40</b>
(2) Limestone	1/3	1									0.229	0.237	0.0543	6	5	30
(3) Banded limestone, sandstone and shale	1/2	2	1								0.198		0.0469	5		25
(4) Igneous	1/7	1/3	1/5	1							0.044		0.0105	4		20
(5) Weathered Metamorphic/igneous	1/5	1/2	1/3	4	1						0.098		0.0232	5		25
<i>Hydraulic conductivity (m/d)</i>																
(1) 0.04075–4.075	1										0.032		0.0021	1		3
(2) 4.075–12.225	2	1									0.047		0.0031	2		6
(3) 12.225–28.525	3	3	1								0.083	0.065	0.0054	4	3	12
(4) 28.525–40.75	5	4	3	1							0.143		0.0094	6		18
(5) 40.75–81.5	7	5	4	3	1						0.243		0.0158	8		24
(6) 81.5<	9	7	6	5	3	1					<b>0.453</b>		<b>0.0294</b>	10		<b>30</b>
<i>Land use classes</i>																
(1) Agricultural area	1										0.192		0.0296			
(2) Arable land	1/2	1									0.135		0.0208			
(3) Forestry	1/4	1/3	1								0.064		0.0099			
(4) Mine, dump site	1/3	1/2	4	1							0.126		0.0194			
(5) Natural grassland	1/3	1/2	1/2	1/3	1						0.046	0.154	0.0071			
(6) Open field	1/5	1/4	1/3	1/5	2	1					0.053		0.0082			
(7) Pasture	1/4	1/3	1/2	1/4	1	2	1				0.055		0.0085			
(8) Settlement	2	3	5	3	4	4	5	1			<b>0.257</b>		<b>0.0396</b>			
(9) Shrub	1/4	1/4	2	1/3	2	1/2	1/2	1/5	1		0.054		0.0083			
(10) Water body	1/7	1/6	1/4	1/4	1/3	1/5	1/4	1/9	1/4	1	0.018		0.0028			

The most important subcriteria and their values are written in bold.

In the AHP-DRASTICLu model, the land use classes parameter, an environmental factor that impacts groundwater pollution, was added to Aller's generic DRASTIC model. The rate and weight values of the main criteria (parameter) and their subcriteria were assigned with the analytical hierarchy process (AHP) method, which is one of the multicriteria decision-making methods. An AHP-DRASTICLu vulnerability index (AHP-DV<sub>i</sub>) map was created by applying Equation (2) on the GIS platform to the rate (r) and weight (w) values calculated by the AHP for each main parameter of the AHP-DRASTICLu model. The methodology used in generic DRASTIC and AHP-DRASTICLu index maps is depicted in Figure 4.

$$DV_i = (D_r \times D_w) + (R_r \times R_w) + (A_r \times A_w) + (S_r \times S_w) + (T_r \times T_w) + (I_r \times I_w) + (C_r \times C_w) \quad (1)$$

$$AHP-DV_i = (D_r \times D_w) + (R_r \times R_w) + (A_r \times A_w) + (S_r \times S_w) + (T_r \times T_w) + (I_r \times I_w) + (C_r \times C_w) + (Lu_r \times Lu_w) \quad (2)$$

### 2.3. Weight Assignment and Normalisation of DRASTICLu Criteria Using AHP

The analytical hierarchy process method [68], which is based on pairwise comparisons in line with expert opinions, provides great convenience in making complex decisions. The first stage of the AHP is determining the necessary criteria in line with the main target and forming pairwise comparison matrices (Equation (3)) of the selected criteria. Thus, the complex decision-making process between the criteria is reduced to a single level, and the

relative importance values of the criteria are obtained. The degree of importance of the criteria against each other is assigned using values ranging from 1 to 9 (Table 5).

$$A = \begin{bmatrix} a_{11} & \cdots & a_{1n} \\ \vdots & \ddots & \vdots \\ a_{n1} & \cdots & a_{nn} \end{bmatrix} \quad (3)$$

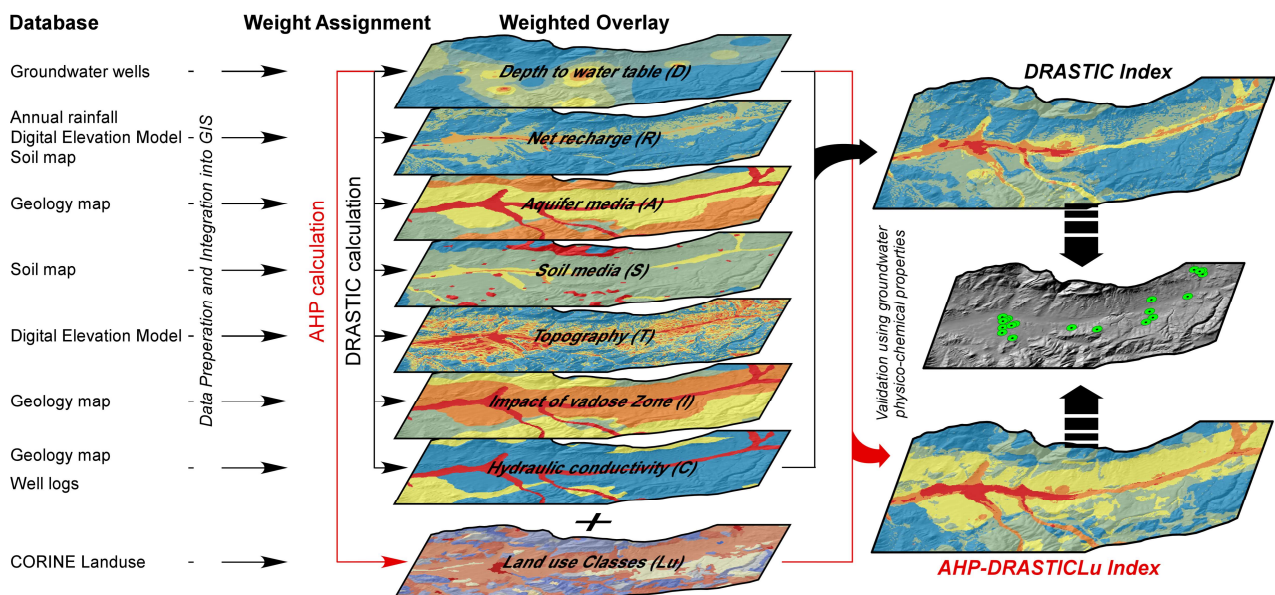


**Figure 4.** Methodology flowcharts for groundwater vulnerability analysis using GIS-based generic DRASTIC and AHP-DRASTICLu models.

**Table 5.** Saaty's 1–9 scale of relative importance.

Scale	Judgment	Explanation
1	Equally	Two criteria contribute equally to the goal
3	Slightly	Criterion 1 is slightly more important than criterion 2
5	Strongly	Criterion 1 is strongly important compared to criterion 2
7	Very Strongly	Criterion 1 is very strongly important compared to criterion 2
9	Extremely	Criterion 1 is extremely important compared to criterion 2
2, 4, 6, 8	Intermediate	Intermediate values between two adjacent numbers

In Equation (3),  $a_n$  shows the  $n$ th indicator unit, and  $a_{nn}$  is the judgment matrix element.

The second stage of the AHP methodology is to define the normalized weights using the geometric mean of the criteria (Equation (4)).

$$W_n = \frac{G_m}{\sum_{n=1}^n G_m} \quad (4)$$

In Equation (4),  $W$  is the eigenvector and  $G_m$  is the geometric mean of the  $i$ th row of the judgment.

The third and final stage of the AHP calculations is to test the consistency of the normalizations of the criteria. The consistency ratio (CR) (Equation (5)) is used in the consistency test. A CR less than 0.10 indicates that the normalized weight values of the criteria are consistent after pairwise comparisons, while a CR greater than 0.10 suggests that paired comparisons should be redesigned.

$$CR = \frac{CI}{RI} \quad (5)$$

In Equation (5),  $CR$  is the consistency ratio,  $CI$  is the consistency index calculated using Equation (6), and  $RI$  is the random consistency index (see Table 6).

$$CI = \frac{\lambda_{max} - n}{n - 1} \quad (6)$$

**Table 6.** Random consistency index ( $RI$ ) ratio of the different values of  $n$  [68].

Order	1	2	3	4	5	6	7	8	9	10
$RI$	0.00	0.00	0.52	0.89	1.11	1.25	1.35	1.40	1.45	1.49

In Equation (6),  $\lambda_{max}$  is the maximum eigenvalue of the judgment matrix, which is calculated using Equation (7).

$$\lambda_{max} = \frac{1}{n} \sum_{i=1}^n \frac{A_i \times w_i}{w_i} \quad (7)$$

The main criteria (8 criteria) of the AHP-DRASTICLu model and pairwise comparison matrices of the subcriteria of these criteria, standardized rating ( $r$ ), and normalized weight ( $w$ ) values are given in Tables 3 and 4. As a result of the consistency tests of the pairwise comparisons of each criterion, it was determined that the  $CR$  values were lower than 0.10, and the values of the consistency test calculations ( $\lambda_{max}$ ,  $CI$ , and  $CR$ ) are given in Table 7.

**Table 7.** The number of criteria and their subcriteria ( $n$ ), maximum eigenvalue of the judgment matrix ( $\lambda_{max}$ ), consistency index ( $CI$ ), random consistency index ( $RI$ ), and consistency ratio ( $CR$ ) for the criteria DRASTICLu model.

Criteria	$n$	$\lambda_{max}$	$CI$	$RI$	$CR$
DRASTICLu	8	8.29	0.041	1.40	0.029
Depth to water table	7	7.52	0.088	1.35	0.065
Net recharge	5	5.25	0.063	1.11	0.056
Aquifer media	5	5.42	0.060	1.11	0.054
Soil media	8	8.82	0.117	1.40	0.083
Topography	5	5.18	0.045	1.11	0.040
Impact of vadose zone	5	5.32	0.080	1.11	0.072
Hydraulic conductivity	6	6.52	0.103	1.25	0.082
Land use classes	10	11.15	0.128	1.49	0.086

#### 2.4. Data Preparation and Integration into a GIS Database

In this study, the basic datasets required to create the eight criteria layers used to determine the aquifer vulnerability to pollution have been obtained from different sources at various scales and resolutions (see Table 8). Each data layer was georeferenced within a GIS environment (ArcGIS 10.3.1) using the UTM projection system (Zone 37N) and WGS84 datum, and all operations (storage, integration, conversion, manipulation, analysis, and visualization) were performed using related plugins (such as 3D Analyst, Spatial Analyst, and Geostatistical Analyst) available in the software. The basic criteria layers in the GIS (D, R, A, S, T, I, C, Lu) used in this study consist of a grid format consisting of cells with a resolution of  $25 \times 25$  m.

The depth to water table refers to the distance from the surface to the groundwater table. The distance values measured in 40 different groundwater wells (Figure 1) scattered in the study area were used as basic data to create the depth to water table (D) layer in the UKV. Vector-based data transferred into the ArcGIS environment in point data format were interpolated using the kriging method, and the study area's depth to water table layer was created. Afterward, this grid layer was reclassified and divided into seven classes, and by assigning rating values (Table 4) to each class, "D" layers were created for the generic DRASTIC and AHP-DRASTICLu models (Figure 5a).

**Table 8.** Time-series and spatial data used to set up and evaluate the DRASTIC and AHP-DRASTICLu models in the Upper Kelkit Valley (UKV).

Data Type	Sources	Format	Period/Date	Produced Parameter
Groundwater wells data	On-site measurement	Table	2022	Depth to water table (D)
Average annual rainfall	Turkish State of Meteorological Service [48]	Table	2003–2021	Rainfall amount for net recharge (R)
Topographical sheets	Turkish Ministry of National Defense General Command of Maps (H42d, H43c, I42b, and I43a)	Map	1989 and 1990	Topography (slope %) for net recharge (R)
Soil map	General Directorate of Rural Services [50]	Map	2001	Soil permeability for net recharge (R)
Geology map	[51]	Map	1993	Aquifer media (A)
Soil texture	General Directorate of Rural Services [50]	Map	2001	Soil media (S)
Topographical sheets	Turkish Ministry of National Defense General Command of Maps (H42d, H43c, I42b, and I43a)	Map	1989 and 1990	Topography (slope %) (T)
Geological profile	[51]	Map	1993	Impact of vadose zone (I)
Geology map and borehole data	[51,63,69]	Map and table	1992, 1993, and 2015	Hydraulic conductivity (C)
Land use map	CORINE Land use land classes [55]	Map	2018	Land use (Lu)

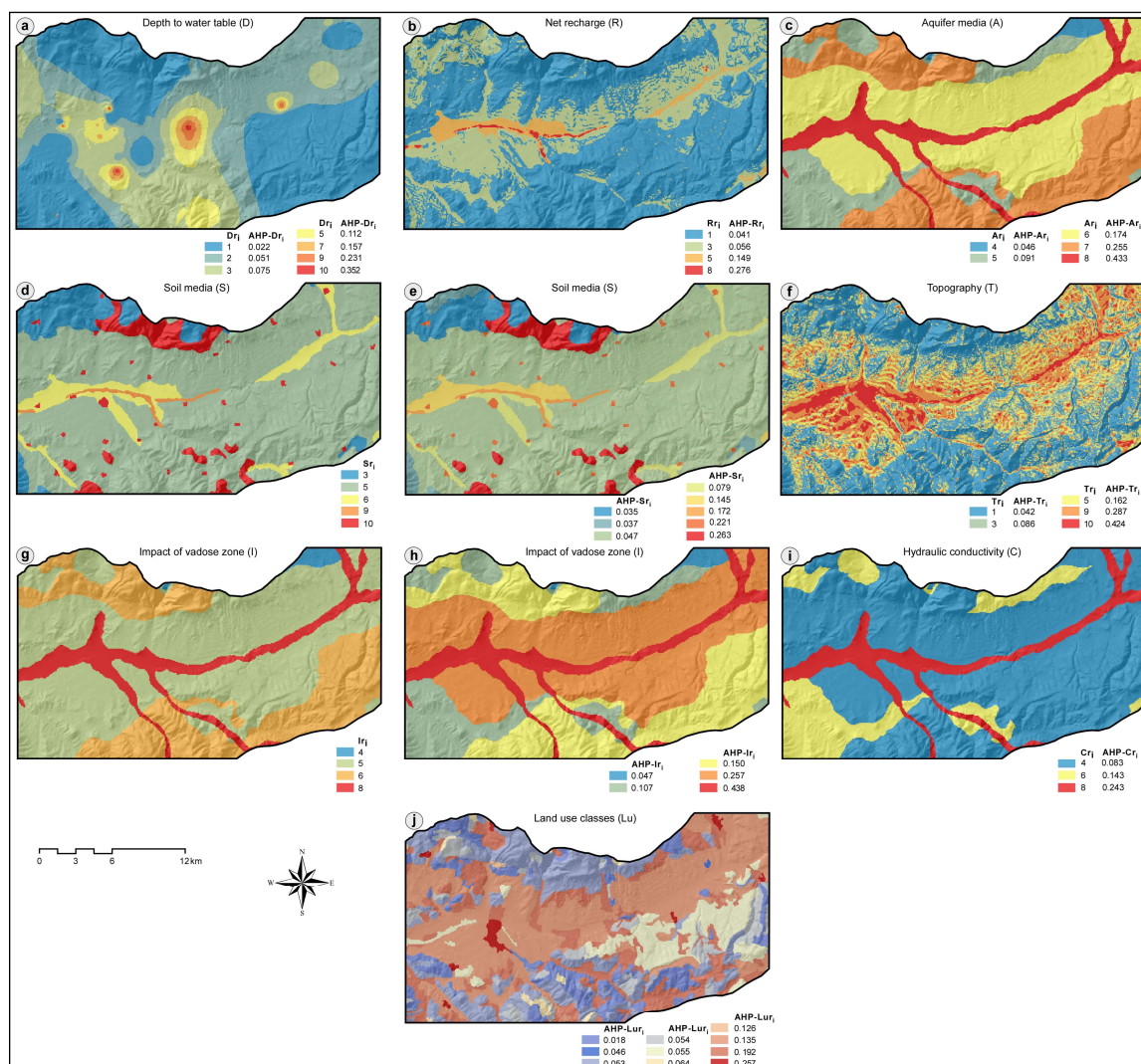


**Figure 5.** Rated thematic maps of UKV's groundwater vulnerability models: (a) depth to water table (D); (b) net recharge (R); (c) aquifer media (A); (d,e) soil media (S); (f) topography (slope %) (T); (g,h) impact of vadose zone (I); (i) hydraulic conductivity (C); (j) land use classes (Lu). ri: generic DRASTIC model rating value; AHP-ri: AHP-DRASTICLu model rating value.

The net recharge represents the annual total amount of water that infiltrates the vadose region and reaches the groundwater table [23]. The net recharge, one of the most important factors in transporting pollutants to groundwater, can be calculated by many different methods. In this study, the net recharge (R) layer of the study area was generated using the technique of Piscopo [70] (Equation (8)).

$$RV = RA + T + SP \quad (8)$$

In Equation (8),  $RV$  is the potential recharge value,  $RA$  is rainfall amount,  $T$  is the topography (slope percentage), and  $SP$  is the soil permeability.

The precipitation amount layer of the study area was created by transferring the annual total average of the precipitation measured between 2003 and 2021 at Kelkit and Köse meteorological stations to the GIS environment. Depending on the precipitation amount of 300 mm/year throughout the study area, the RA value was assigned to the relevant criterion layer as “1” according to Table 9. The topography layer has been derived from the digital elevation model of the study area using the 3D analysis plugin in the ArcGIS environment.

**Table 9.** The criteria used in estimating the recharge potential according to Piscopo’s [70] method, the ranges of the criteria, and the weights of these ranges.

Rainfall Amount (mm/yr)		Topography (% Slope)		Soil Permeability		Recharge Value (RV—Unitless)		
Range	Rate	Range	Rate	Range	Rate	Range	Rate	Definition
>850	4	<2	4	High	5	11–13	10	Very High
700–850	2	2–10	3	Moderately High	4	9–11	8	High
500–700	2	10–33	2	Moderate	3	7–9	5	Moderate
<500	1	>33	1	Low	2	5–7	3	Low
				Very Low	1	3–5	1	Very Low

The digital elevation model of the study area was created by the “topo to raster conversion” plugin, which is available in ArcGIS, using vector data produced by digitizing the isohips of maps H42d, H43c, I42b, and I43a published by the Turkish Ministry of National Defense General Command of Maps. Afterward, this topography layer was divided into four different classes, as shown in Table 9. The T layer required for RV calculation was created by assigning the relevant rating value to the classes in the relevant range.

The soil permeability layers of the study area were obtained by digitizing the 1/25,000 scaled soil characteristics map of Turkey [50] in the ArcGIS environment. Depending on the texture characteristics of the soil types in the study area [71–73], they were divided into five classes: high, moderately high, moderate, low, and very low in terms of permeability. Then, the SP layer of the study area was created by assigning the rating values of each class (Table 9) to the relevant cells.

Finally, these RA, T, and SP layers were collected by the raster calculator plugin in ArcGIS, as shown in Equation (8). The last layer obtained was reclassified according to the RV ranges shown in Table 9. Then, “R” layers were created for the generic DRASTIC and AHP-DRASTICLu models by assigning the relevant rating values (Table 4) to the class ranges (Figure 5b).

The aquifer media represent the consolidated or unconsolidated material that forms the aquifer in the saturated zone [23]. The aquifer media (A) layer of the study area has been derived from the lithological units represented by the formations indicated in the 1/25,000-scaled geological map of the region [51]. The layer created in vector format with digitization in the ArcGIS environment was converted into the grid format with the help of the “feature to raster” plugin, and the “A” layers were created for the generic DRASTIC and AHP-DRASTICLu models by assigning the rating values (Table 4) to the relevant classes (Figure 5c).

The soil media (S) represent the uppermost layer of the vadose zone and are one of the most important control mechanisms in water infiltration into the ground and groundwater

recharge [23,74]. The UKV's soil media (S) layer was derived from the 1/25,000-scaled soil characteristics map of Turkey [50] in vector format. Soil classes in the study area were classified according to the texture properties (clay loam for noncalcic brown forest and brown forest soils; loam for brown soil; sand for floodplain; sandy loam for alluvium and colluvium; thin or absent for settlement and bare rock) specified in some studies in the literature [71–73]. Afterward, this layer was converted into the grid format in the ArcGIS environment, and the soil media (S) layers of the study area were created for both models by assigning the rating values shown in Table 4 to the relevant classes (Figure 5d,e).

Topography refers to the slope of the land surface. The digital elevation model of the study area was used to create the topography (T) layers for the models of the UKV. Using the digital elevation model, the slope map was created with the help of the 3D Analysis tool in the ArcGIS software. Then, the slope map was divided into the classes indicated in Table 4, and the study area's topography (T) layers were created by assigning the rating values to the relevant classes (Figure 5f).

The vadose zone refers to the unsaturated or discontinuously saturated region between the groundwater table and the soil horizon [27]. The vadose zone material is one of the most significant mechanisms controlling transit time and the amount of pollutants and water leaking into the groundwater from the land surface [23]. The impact of the vadose zone (I) layers in the UKV has been derived using the vadose zone materials specified in the geological map of the study area [51]. The layer in vector format was converted into the grid format, then the "I" layers of the study area were created by assigning the rating values shown in Table 4 to the relevant classes (Figure 5g,h).

The hydraulic conductivity (C) is the capacity of the aquifer to transmit water [75]. The hydraulic conductivity layer of the UKV has been derived from lithological units [51,63] and well logs obtained from geotechnical studies [69] in the study area. The "C" layer of the study area was created by converting the layer in vector format into the grid format and assigning the rating values shown in Table 4 to the relevant classes (Figure 5i).

CORINE [55] land use land classes (LULCs) data in grid format were used as the basic data to create the land use classes (Lu) layer of the study area. The "Lu" layer of the study area was formed by assigning the rating values shown in Table 4 to the relevant classes (Figure 5j).

## 2.5. Comparison and Validation of Generic DRASTIC and AHP-DRASTICLu Models

The similarity analysis of the generic DRASTIC and AHP-DRASTICLu model maps of the study area has been conducted by pairwise statistical comparisons under the Spearman correlation method [76]. In addition, the groundwater vulnerability indexes of both models have been validated with the Spearman correlation method using the sulfate, chloride, nitrate, and electrical conductivity of the groundwater samples collected from 20 wells (Figure 6) in the study area in November 2022 and the vulnerability index values belonging to the well locations.

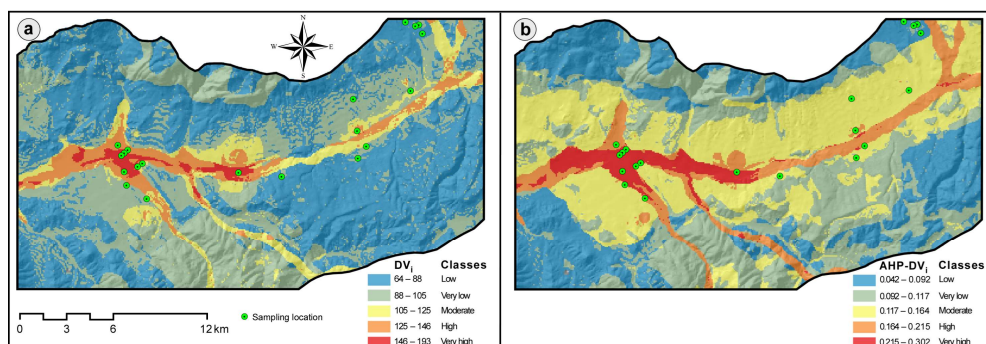


**Figure 6.** Classified groundwater vulnerability index (DV<sub>i</sub>) maps of the Upper Kelkit Valley (UKV): (a) generic DRASTIC model; (b) AHP-DRASTICLu model.

## 2.6. Sensitivity Analysis

An effective assessment tool is sensitivity analysis, which examines the contribution of individual variables and input parameters to the resultant output of an analytical model [77]. The sensitivity analysis validates and evaluates the uniformity of the analytical results of vulnerability maps [77]. It provides an efficient foresight to identify the most effective indicators of vulnerability and then explore how to deal with pollution and aquifer crisis management. In this study, the single-parameter sensitivity analysis, first introduced by Napolitane and Fabbri [77], was applied to check the accuracy of the vulnerability maps created by the DRASTIC and AHP-DRASTICLu models.

Single-parameter sensitivity analysis aims to compare the effective weights of different parameters with the theoretical weights assigned by the corresponding model [27]. The effective weight of each parameter was calculated by Equation (9) [77]:

$$W = (P_r \times P_w / V) \times 100 \quad (9)$$

In Equation (9),  $W$  is the effective weighting of each parameter,  $P_r$  and  $P_w$  are the rating and weighting values of each parameter, respectively, and  $V$  is the overall vulnerability index.

## 3. Results and Discussion

### 3.1. Weighted Thematic Maps of the Criteria

The distances from the surface to the water table in the UKV vary between 0.5 m and 99.9 m. According to the generic DRASTIC method [23], the “Depth to water table” classes and covered areas in the UKV are 0.07% for 0–1.52 m, 0.42% for 1.52–4.57 m, 1.09% for 4.57–9.14 m, 9.14–4.88% for 15.24 m, 20.06% for 15.24–22.86 m, 29.72% for 22.86–30.48 m, and 43.76% for 30.48 m. Shallow depths (with relatively high rating values) are observed around the Kelkit Stream flowing east to west of the study area. In contrast, the classes with the deeper parts (with relatively low rating values) are topographically higher regions in the northern and southern parts of the study area (Figure 5a).

The depth to groundwater table indicates the distance at which the surface-borne pollutants will reach the groundwater, and groundwater is more vulnerable to pollution in areas with low distances [78]. Water and pollutants travel a longer pathway to reach the groundwater table in deeper groundwater table environments. This case allows more time for the pollutant to detoxify as it flows through the soil layers, indicating groundwater is less vulnerable to pollution [79]. In generic DRASTIC and AHP-DRASTICLu models, classes with low distances from the surface to groundwater have higher weight values, while classes with greater distance have lower weight values (Table 4).

Medium and high net recharge (R) classes are observed in the regions where the alluvial units formed by the Kelkit Stream accumulating the fragments that tore from the surrounding rocks around its bed, whereas the other parts generally have a very low net recharge, class “R” values (Figure 5b). In both groundwater vulnerability models established for the UKV, low net recharge (R) classes have low weight values, whereas high net recharge classes have high weight values (Table 4). While 66.41% of the study area is represented by the very low net recharge (R) class, 29.24% is in the low class, 3.78% is in the medium class, and 0.57% is in the high class. The amount of recharge water leaking to the aquifer affects the amount of pollutants transported to the aquifer [80]. The higher the recharge water amount, the higher the vulnerability of groundwater to pollution and vice versa [81].

The geological formations in the study area were divided into “Alluvium”, “Massive limestone”, “Badded sandstone, limestone and shale”, and “Igneous and Weathered metamorphic/igneous” classes according to the aquifer media (A) classification in the generic DRASTIC method in terms of their lithological properties. These classes cover 11.18%, 28.36%, 44.01%, 1.16%, and 15.30% of the study area, respectively.

The aquifer media classes in the UKV are as follows: the alluvial aquifer, by the alluvium units located around the Kelkit Stream; the “Badded sandstone, limestone, and

shale” aquifer, by the conglomerate, sandstone, sandy limestone, shale, and tuff, which surround the alluvial aquifer and are referred to as the Kelkit Formation in the region; the “Massive limestone” aquifer, by the limestones of the Berdiga Formation, which is a karstic aquifer cropping out in topographically higher areas in the study area; the “Igneous” aquifer, by the granites covering a relatively small area in the northeast of the study area; and the “Weathered metamorphic/igneous” aquifer, by the “Senkoy Formation” units, which cover areas in the northern and southern parts of the study area, which generally consist of basaltic and pyroclastic rocks with abundant cracks and fractures (Figures 2d and 5c). While the alluvium aquifer class has the highest weight value in the aquifer media criterion for both models, the lowest value belongs to the “igneous” aquifer class (Table 4). The flow path of water below the surface is controlled by factors such as the hydraulic conductivity of the aquifer and gradient [82]. Since the fine-grained and low-permeability aquifer material is more resistant to the infiltration of pollution into the aquifer, the pollution vulnerability is lower in these systems.

The most common soil class in the UKV is brown soil with a loam texture, which covers approximately 3/4 of the study area. This class, which has a rating of “5” according to the generic DRASTIC method, has a rating of “0.047” according to the AHP-DRASTICLu model (Table 4). The rest of the soil classes with areas they cover in the UKV are noncalcareous brown forest and brown forest soil with a clay loam texture of 6%, floodplain with a sand texture of 0.94%, alluvium and colluvium with a sandy loam texture of 7.72%, and bare rock and settlement represented by thin or absent classes of 6.21%. In soils with more coarse-grained materials, such as sand and gravel, the water infiltration capacity will be higher, and the vulnerability of groundwater to pollution is higher in these systems [83]. However, the presence of organic materials, such as clay and organic matter, creates resistance against water infiltration to the ground, reducing pollution vulnerability in groundwater [33,84]. Among the soil classes in the UKV, the highest vulnerability rating value belongs to the bare rock and settlement classes, represented by “thin or absent” for both models. In contrast, the lowest rating values are for noncalcareous brown forest and brown forest soils depicting the clay loam texture spread in different regions of the UKV (Table 4 and Figure 5d,e).

The topography layer of the UKV was classified into five groups according to land slope (%) ranges: 0–2%, 2–6%, 6–12%, 12–18%, and >18%. These classes occupy the areas of 6.28%, 18.61%, 21.08%, 15.02%, and 39.01% in the UKV, respectively (Table 1). The topography criterion is one of the most critical factors controlling the water residence time on the land surface [85]. In the land with a low slope, the water stays on the surface longer, so the amount of surface water infiltrating underground will be greater. Thus, the amount of pollutants that can leak into the groundwater also increases [81]. In the northern and southern parts of the study area, the slope of the land is high in topographically high regions, and the rating values of the topography classes are low in both generic DRASTIC and AHP-DRASTICLu models in these areas (Figure 5f). In the middle parts of the study area, the land slopes along the east–west extension belt are lower, and the topography class rating values are higher for both models in these areas (Figure 5f).

The vadose zone materials in the UKV were grouped into five different classes, namely “Alluvium”, “Massive limestone”, “Banded limestone, sandstone and shale”, “Igneous”, and “Weathered Metamorphic/igneous”, as specified in the DRASTIC method. These classes cover 11.18%, 28.36%, 44.01%, 1.15%, and 15.30% of the UKV, respectively. The fact that the vadose zone consists of units with a high permeability, such as sand and gravel, allows pollutants to reach the groundwater in larger quantities and in a shorter time. This situation indicates that the vulnerability of groundwater to pollution in these regions is higher [23]. Among the vadose zone classes in the UKV, the most vulnerable class for groundwater pollution is “Alluvium”, and the rating values are “8” for the generic DRASTIC model and “0.438” for the AHP-DRASTICLu model. In contrast, the class with the lowest vulnerability is “Igneous”, and the rating value of this class is “4” for the generic DRASTIC model and “0.047” for the AHP-DRASTICLu model (Figure 5g,h).

The movement of water and pollutants through the aquifer is greatly affected by hydraulic conductivity. The higher the hydraulic conductivity of an aquifer, the more pollutants could be transmitted to groundwater and, therefore, the higher the groundwater vulnerability to pollution [10,33,85]. The hydraulic conductivity values of the UKV were classified into three different classes: 12.225–28.525 m/d, 28.525–40.75 m/d, and 40.75–81.5 m/d. While the highest hydraulic conductivity class has the highest rating values of vulnerability for both the generic DRASTIC (8) and AHP-DRASTICLu (0.243) models, the class with the lowest hydraulic conductivity values has the lowest ratings for both models (4 for the DRASTIC and 0.083 for the AHP-DRASTICLu) (Table 4). The areas with the highest hydraulic conductivity rating values and, therefore, the areas most vulnerable to pollution in terms of hydraulic conductivity, are located around the Kelkit Stream, which is the main stream of the study area (Figure 5i). This class covers 11.17% of the study area. However, the lowest vulnerable areas in terms of hydraulic conductivity cover approximately 3/4 of the UKV.

Land use classes can be a source of pollutants and can control the way water [86] and pollutants reach the groundwater [10,87,88]. Anthropogenic effects, such as domestic and industrial wastes, improper design of septic tanks, and agricultural activities, especially pesticides, may affect the groundwater quality and cause it to become polluted [38]. A large part of the UKV consists of farming activity classes (35.5% of UKV is arable land, and 17.7% of UKV is agricultural area), and these classes are located at the central part of the study area along an east–west extending belt with a low land slope (Figure 3d). These classes are highly vulnerable to pollution, and the rating values in the AHP-DRASTICLu model are “0.192” for “agricultural area” and “0.135” for “arable land” (Table 4). The highest rating value of the land use classes criteria belongs to the settlement with “0.257”. The rating values for the other land use classes, “forestry”, “mine, dump site”, “natural grassland”, “open field”, “pasture”, “shrub”, and “water body”, are “0.064”, “0.126”, “0.046”, “0.053”, “0.055”, “0.054”, and “0.018”, respectively (Table 4). The spatial distributions of rated land use classes are shown in Figure 5j.

### 3.2. The Groundwater Vulnerability Maps of DRASTIC and AHP-DRASTICLu Models

“Depth to water table”, “Net recharge”, and “Impact of vadose zone” criteria, compared to the other criteria used in the DRASTIC and AHP-DRASTICLu models, in addition to the “Land use” criterion with its impact in AHP-DRASTICLu model, are more decisive factors on groundwater vulnerability to pollution according to their theoretical weights. Many previous studies have shown that these criteria are dominant factors in groundwater vulnerability to pollution [10,31,33,88]. The generic DRASTIC index ( $DV_i$ ) values of the study area obtained as a result of the analysis range between “64” and “193”, and the AHP-DRASTICLu index (AHP- $DV_i$ ) values vary between “0.042” and “0.302” (Figure 6). These vulnerability index maps of the UKV were reclassified into five categories (very high vulnerability, high vulnerability, moderate vulnerability, low vulnerability, and very low vulnerability) to help better understand the spatial distribution patterns of the different vulnerability categories. The areal distributions (% area of the UKV) of these classes were 1.42%, 5.48%, 7.80%, 34.31%, and 50.98%, respectively, according to the generic DRASTIC vulnerability index classification, and they were 3.90%, 8.02%, 31.78%, 29.86%, and 26.44%, respectively, according to the AHP-DRASTICLu vulnerability index classification.

As a result of both models, classes with high to very high vulnerabilities were observed along the east–west belt formed along the Kelkit Stream in the study area (Figure 6). The areas represented by these classes are generally land use classes related to farming activity with a very low topographic slope (with averages of 2° for the DRASTIC model and 4° for AHP-DRASTICLu model), dominated by alluvium and floodplain soil classes and areas with relatively shallow water table depths where residential areas are the dominant land use classes. Similar results were reported in the previous studies on groundwater vulnerability in northern Turkey [85] and in the arid/semi-arid regions with climatic conditions similar to the UKV [33,67,89].

The moderate vulnerability class of the AHP-DRASTICLu model covers a larger area than the DRASTIC model. These classes mainly extend to the high vulnerability class borders with the east–west trending hills in the northern and southern parts of the study area, where the topographical slope begins to increase relatively. The average slope of the moderate vulnerability class of the DRASTIC model is  $7^\circ$ , while it is  $6^\circ$  in the AHP-DRASTICLu model. The dominant aquifer type in these areas consists of clastic rocks containing fine-grained materials. The predominant soil class is “brown soil”, and the most common land use classes are “arable land” and “agricultural area” in the moderate vulnerability areas of the UKV.

In the northern and southern parts of the study area, the vulnerability varies from low to very low on the east–west trending hill range, where the topographic heights and slopes are relatively high (Figure 6). In areas representing this class, the distances to the groundwater table are relatively greater (an average of 34 m for the DRASTIC model, and an average of 38 m for the AHP-DRASTICLu model).

### 3.3. Models' Comparison and Validation

In order to test the accuracy of the vulnerability index maps obtained, 20 different groundwater samples scattered over the area in November 2022 were gathered (Figure 6), and their physicochemical contents were analyzed. The analysis results and vulnerability index values were compared using the Spearman correlation method.

The sulfate concentrations of the groundwater samples collected from the study area varied from 15.12 mg/L to 115.14 mg/L, the chloride concentrations of the samples ranged between 4.89 mg/L and 58.63 mg/L, the nitrate concentrations of the samples ranged between 0.51 mg/L and 200.45 mg/L, and the electrical conductivity values ranged between 499  $\mu\text{S}/\text{cm}$  and 1450  $\mu\text{S}/\text{cm}$ . While calcium sulfates, such as gypsum and anhydrite, are the most common sources of sulfates in natural waters, barium sulfates, strontium sulfates, the oxidation of pyrite minerals, volcanoes, geothermal fields, the burning of fossil fuels, and the oxidation of sulfates in soil or organic wastes are also sources of sulfate in natural water [90,91]. Apart from these factors, the sulfate concentration in surface water and groundwater may increase due to industrial and domestic wastes and sulfate-containing fertilizers used in agriculture [92–94]. Chloride leaching from chemical fertilizers in agricultural soils or wastewater discharged to the land surface may increase the chloride concentration in groundwater [95]. The most common nitrate sources in groundwater are inorganic and organic fertilizers used in agricultural activities, organic materials in the soil, industrial wastes, solid waste disposal areas, highways, and sewage waters [96–98]. The electrical conductivity of water represents the dissolved ion concentration in the water. The dissolved ion concentration in water with high electrical conductivity is high and vice versa [90,99].

As a result of the correlation analysis, it was observed that there was a strong correlation between the vulnerability index values of both models and the sulfate, chloride, and electrical conductivity contents of the groundwater samples, whereas the nitrate values and vulnerability index values were not correlated. In the UKV, the correlation coefficients between sulfate concentrations of groundwater samples and generic DRASTIC and AHP-DRASTICLu index values are “0.661” and “0.752”, respectively; the correlation coefficients between chloride concentrations and generic DRASTIC and AHP-DRASTICLu index values are “0.684” and “0.758”, respectively; the correlation coefficients between nitrate concentrations and generic DRASTIC and AHP-DRASTICLu index values are “−0.245” and “−0.151”, respectively; and the correlation coefficients between the electrical conductivity and DRASTIC and AHP-DRASTICLu index values are calculated as “0.678”, and “0.652”, respectively (Table 10). The correlation coefficient between the DRASTICLu index values and the generic DRASTIC index values is “0.931”. Considering the correlation analysis results, it was seen that the AHP-DRASTICLu model provides more accurate results than the DRASTIC model in terms of the sulfate and chloride contents of the groundwater except for the electrical conductivity in the UKV.

**Table 10.** The Spearman correlation results between sulfate concentrations, chloride concentrations, nitrate concentrations, electrical conductivity, and aquifer vulnerability maps: DRASTIC index and AHP-DRASTICLu index.

	DRASTIC	AHP-DRASTICLu
DRASTIC	1	
AHP-DRASTICLu	0.931	1
Sulfate	0.661	0.752
Chloride	0.684	0.758
Nitrate	-0.245	-0.151
Electrical conductivity	0.678	0.652

In many studies conducted to determine the groundwater vulnerability to pollution, the nitrate [31,100,101], sulfate [102–104], and chloride [29,105] concentrations of groundwater were used to validate the model results. It was seen that the vulnerability index values were highly correlated with sulfate in some areas [106,107], chloride in some areas [35,108], and nitrate in some areas [36,109]. These differences suggest groundwater vulnerability models respond differently in different climatic and hydrogeoenvironmental areas.

### 3.4. Single-Parameter Sensitivity Analysis

Single-parameter sensitivity analysis compares “theoretical” and “effective” weights. Here, the effective weight is a function of the value of the single parameter compared to other parameters and the weight the model assigns [27]. The effective weights of the parameters of the DRASTIC and AHP-DRASTICLu models have deviated from theoretical weights (Table 11). In the DRASTIC and AHP-DRASTICLu models, the impact of the vadose zone parameter has a higher effective weight value (30.11% and 40.64%, respectively) than the other parameter, as well as a higher value than the relevant theoretical weights. It is seen that the impact of the vadose zone parameter is the most influential parameter for the sensitivity assessment. Further, the effective weights of aquifer media (10.83%) and hydraulic conductivity (15.34%) parameters in the DRASTIC model and the aquifer media parameter (13.74%) in the AHP-DRASTICLu model show higher values than their theoretical weights (Table 11). The effective weights of all other layers are lower than their theoretical weights. These results show that the impact of the vadose zone parameter has a very important role in both models, and it is important to obtain accurate and detailed information on this factor. In addition, the high effective weight value (14.55%) of the land use classes parameter in the AHP-DRASTICLu model has shown that including this parameter in the model is quite accurate.

**Table 11.** Statistical summary of single-parameter sensitivity analysis.

	Theoretical Weight	Theoretical Weight %	Effective Weight %			
			Mean	Min	Max	Mean
<b>DRASTIC</b>						
D	5	21.73	9.81	3.34	41.43	5.21
R	4	17.39	6.85	2.51	26.35	4.03
A	3	13.04	20.10	11.55	26.12	2.05
S	2	8.69	10.83	5.86	27.48	3.14
T	1	4.34	3.72	0.13	13.92	3.03
I	5	21.73	30.11	15.38	37.49	3.71
C	3	13.04	15.34	7.52	24.67	3.52

**Table 11.** *Cont.*

	Theoretical Weight	Theoretical Weight %	Effective Weight %		
			Mean	Min	Max
<b>AHP-DRASTICLu</b>					
D	0.248	24.82	9.39	2.63	47.26
R	0.1143	14.31	6.27	2.34	32.19
A	0.081	8.14	13.74	3.45	24.74
S	0.047	4.71	2.32	0.49	23.12
T	0.024	2.40	2.31	0.32	19.72
I	0.237	23.71	40.64	10.27	59.37
C	0.065	6.50	6.28	2.92	14.38
Lu	0.154	15.41	14.55	1.69	51.39
					8.01

#### 4. Conclusions

In the present study, the groundwater vulnerability maps of the Upper Kelkit Valley (UKV) have been derived using the generic DRASTIC model and the AHP-DRASTICLu model, which is a modified model that adds the land use class criterion and the weighting of the criteria by the analytical hierarchy process method. According to the vulnerability index values obtained from both models, the study area was reclassified into five classes: very low, low, moderate, high, and very high vulnerability. Considering the spatial distributions of the vulnerability index, the areas covered by the very high, high, and moderate vulnerability classes in the AHP-DRASTICLu model index map in the UKV are larger than in the generic DRASTIC model index map. Both models show that the high to very high vulnerability classes are extended along a belt around the Kelkit Stream in the middle parts of the study area. In contrast, the lower vulnerability classes fall in the areas where the distance to the groundwater is relatively higher, along the east–west trending hills in the north and south of the study area. Particularly, the high and very high vulnerability classes are the areas around the Kelkit district, which is the largest settlement of the study area and where agricultural activities are intense. Considering these factors create a high pollution potential for groundwater, it is recommended that water and land use management planning should be more careful with an integrated management plan by all related persons, institutions, and groups, from water users to decision makers.

In order to validate the model results, the physicochemical contents of the water samples taken from different groundwater wells scattered in the study area and the vulnerability index values of each well location were statistically compared using the Spearman correlation method. The comparison results showed a strong correlation between the groundwater samples' electrical conductivity, sulfate, and chloride concentrations and the vulnerability indexes of both models. In addition, the correlation results showed that the AHP-DRASTICLu model is more accurate than the generic DRASTIC model for groundwater vulnerability assessment of the UKV. Furthermore, the sensitivity analysis revealed that the impacts of the vadose zone, aquifer media, and land use are the most influential parameters responsible for the highest variation in the vulnerability index. These parameters are significant factors as they have a principal role in determining accurate and detailed information for water and environmental planning.

The AHP method reduces the bias due to standard weights in the generic DRASTIC model when combined with the DRASTIC model, one of the most effective methods for vulnerability estimation in groundwater. In addition, adding the land use criterion to the model simulates better the pressures that may cause groundwater pollution. In this sense, with the AHP-DRASTICLU model used in this study, the groundwater vulnerability map for the study area was simulated to be closer to the actual pollution vulnerability.

The fact that the AHP-DRASTICLu model, which was established by modifying the generic DRASTIC model, provides more accurate results indicated that the AHP-DRASTICLu model could be used more efficiently instead of the generic DRASTIC model. However, the AHP-DRASTICLU model may give different results in different climatic and

hydrogeoenvironmental areas. Therefore, AHP analyses should be rearranged according to regional conditions.

**Funding:** This work was supported by the Research Fund of the Bayburt University, Project Number: 2022/69002-13.

**Data Availability Statement:** The hydrological and hydrogeologic input data used for the DRASTIC and AHP-DRASTICLu models presented in this study are available upon request from the author.

**Acknowledgments:** I used the Past 4.11 version software for the correlation analysis.

**Conflicts of Interest:** The author declares no conflict of interest.

## References

1. UNEP—United Nations Environment Programme. Adaptation Gap Report. Nairobi. 2021. Available online: <https://www.unep.org/resources/adaptation-gap-report-2021> (accessed on 6 November 2022).
2. Cramer, W.; Guiot, J.; Fader, M.; Garrabou, J.; Gattuso, J.P. Climate change and interconnected risks to sustainable development in the Mediterranean. *Nat. Clim. Chang.* **2018**, *8*, 972–980. [CrossRef]
3. Şen, Ö.L. *A Holistic View of Climate Change and Its Impacts in Turkey*; Istanbul Policy Center, Sabancı University, Stiftung Mercator Initiative: Istanbul, Turkey, 2013.
4. Reinecke, R.; Schmied, H.M.; Trautmann, T.; Andersen, L.S.; Burek, P.; Flörke, M.; Gosling, S.N.; Grillakis, M.; Hanasaki, N.; Koutroulis, A.; et al. Uncertainty of simulated groundwater recharge at different global warming levels: A global-scale multi-model ensemble study. *Hydrol. Earth Syst. Sci.* **2021**, *25*, 787–810. [CrossRef]
5. WWAP. *The United Nations World Water Development Report 3: Water in a Changing World*; World Water Assessment Programme; UNESCO: Paris, France, 2009.
6. Siebert, S.; Burke, J.; Faures, J.M.; Frenken, K.; Hoogeveen, J.; Döll, P.; Portmann, F.T. Groundwater use for irrigation—A global inventory. *Hydrol. Earth Syst. Sci.* **2010**, *14*, 1863–1880. [CrossRef]
7. Rushton, K.R. *Groundwater Hydrology: Conceptual and Computational Models*; Wiley: Chichester, UK, 2003.
8. Marsala, R.Z.; Capri, E.; Russo, E.; Bisagni, M.; Colla, R.; Lucini, L.; Gallo, A.; Suciu, N.A. First evaluation of pesticides occurrence in groundwater of Tidone Valley, an area with intensive viticulture. *Sci. Total Environ.* **2020**, *736*, 139730. [CrossRef]
9. Bexfield, L.M.; Kenneth, B.; Lindsey, B.D.; Toccalino, P.L.; Nowell, L.H. Pesticides and pesticide degradates in groundwater used for public supply across the United States: Occurrence and human-health context. *Environ. Sci. Technol.* **2021**, *55*, 362–372. [CrossRef] [PubMed]
10. Güler, C.; Kurt, M.A.; Alpaslan, M.; Akbulut Camuzcuoğlu, C. Assessment of the impact of anthropogenic activities on the groundwater hydrology and chemistry in Tarsus coastal plain Mersin SE Turkey using fuzzy clustering multivariate statistics and GIS techniques. *J. Hydrol.* **2012**, *414*, 435–451. [CrossRef]
11. United Nations Committee on Economic Social and Cultural Rights. General Comment No. 15 (2002). In *The Right to Water*; E/C.12/2002/11; United Nations Social and Economic Council: Geneva, Switzerland, 2003; 18p.
12. UN DESA. The Sustainable Development Goals Report 2022. New York, USA. 2022. Available online: <https://unstats.un.org/sdgs/report/2022/> (accessed on 21 February 2023).
13. EU Water Framework Directive: Directive 2000/60/EC of the European Parliament and of the Council Establishing a Framework for the Community Action in the Field of Water Policy. Available online: <https://eur-lex.europa.eu/eli/dir/2000/60/oj> (accessed on 6 November 2022).
14. United Nations. *Johannesburg Plan of Implementation of the World Summit on Sustainable Development*; United Nations: Geneva, Switzerland, 2002; 72p.
15. United Nations. *World Water Development Report 2: Water, a Shared Responsibility*; UNESCO: Paris, France, 2006; 601p.
16. World Water Council. *Final Report of the 4th World Water Forum*; National Water Commission of Mexico: Mexico City, Mexico, 2006; 262p.
17. Margat, J. *Vulnérabilité des Nappes d'eau Souterraine à la Pollution: Bases de la Cartographie*; BRGM Publication No. 68 SGL 198 HYD; BRGM (Bureau de Recherches Géologiques et Minières): Orléans, France, 1968.
18. Evans, B.M.; Myers, W.L. A GIS-based approach to evaluating regional groundwater pollution potential with DRASTIC. *J. Soil Water Conserv.* **1990**, *45*, 242–245.
19. Van Steemvoort, D.; Ewert, L.; Wassenaar, L. Aquifer vulnerability index: GIS-compatible method for groundwater vulnerability mapping. *Can. Water Resour. J.* **1993**, *18*, 25–37. [CrossRef]
20. Hiscock, K.M.; Lovett, A.A.; Brainard, J.S.; Parfitt, J.P. Groundwater vulnerability assessment: Two case studies using GIS methodology. *Q. J. Eng. Geol. Hydrogeol.* **1995**, *28*, 179–194. [CrossRef]
21. Civita, M.; De-Regibus, C. Sperimentazione di alcune metodologie per la valutazione della vulnerabilità degli aquiferi. In *Quaderni di Geologia Applicata, Pitagora Edition*; Pitagora Editrice: Bologna, Italy, 1995.

22. Foster, S.S.D. Fundamental concepts in aquifer vulnerability, pollution risk and protection strategy. In *Vulnerability of Soil and Groundwater to Pollutants*; Duijvenbooden, W., Waagening, H.G., Eds.; Committee on Hydrological Research: The Hague, The Netherlands, 1987; pp. 69–86.
23. Aller, L.; Lehr, J.; Petty, R. *DRASTIC: A Standardized System to Evaluate Groundwater Pollution Potential Using Hydrogeologic Settings*; Bennett, T., Ed.; National Water Well Association: Worthington, OH, USA; Bennett and Williams, Inc.: Columbus, OH, USA, 1987; 43229p.
24. Doerfliger, N.; Jeannin, P.Y.; Zwahlen, F. Water vulnerability assessment in karst environments: A new method of defining protection areas using a multi-attribute approach and GIS tools (EPIK method). *Environ. Geol.* **1999**, *39*, 165–176. [CrossRef]
25. Goldscheider, N.; Klute, M.; Sturm, S.; Hötzl, H. The PI method—A GIS-based approach to mapping groundwater vulnerability with special consideration of karst aquifers. *Z. Für Angew. Geol.* **2000**, *46*, 157–166.
26. Vias, J.M.; Andrea, B.; Perles, M.J.; Carrasco, F.; Vadillo, I.; Jimenez, P. Proposed method for groundwater vulnerability mapping in carbonate (Karstic) aquifers: The COP Method. *Hydrogeol. J.* **2006**, *14*, 912–925. [CrossRef]
27. Babiker, I.S.; Mohamed, M.A.A.; Hiyama, T.; Kato, K. A GIS-based DRASTIC model for assessing aquifer vulnerability in Kakamigahara Heights, Gifu Prefecture, central Japan. *Sci. Total Environ.* **2005**, *345*, 127–140. [CrossRef] [PubMed]
28. Rahman, A.A. GIS based DRASTIC model for assessing groundwater vulnerability in shallow aquifer in Aligarh, India. *Appl. Geogr.* **2008**, *28*, 32–53. [CrossRef]
29. Güler, C.; Kurt, M.A.; Korkut, R.N. Assessment of groundwater vulnerability to nonpoint source pollution in a Mediterranean Coastal Zone (Mersin, Turkey) under conflicting Landuse practices. *Ocean Coast. Manag.* **2013**, *71*, 141–152. [CrossRef]
30. Pacheco, F.A.L.; Sanches Fernandes, L.F. The multivariate statistical structure of DRASTIC model. *J. Hydrol.* **2013**, *476*, 442–459. [CrossRef]
31. Wei, A.; Bi, P.; Guo, J.; Lu, S.; Li, D. Modified DRASTIC model for groundwater vulnerability to nitrate contamination in the Dagujia river basin, China. *Water Supply* **2021**, *21*, 1793–1805. [CrossRef]
32. Maqsoom, A.; Aslam, B.; Khalil, U.; Ghorbanzadeh, O.; Ashraf, H.; Faisal Tufail, R.; Farooq, D.; Blaschke, T. A GIS-based DRASTIC model and an adjusted DRASTIC model (DRASTICA) for groundwater susceptibility assessment along the China–Pakistan Economic Corridor (CPEC) Route. *ISPRS Int. J. Geo Inf.* **2020**, *9*, 332. [CrossRef]
33. Mkumbo, N.J.; Mussa, K.R.; Mariki, E.E.; Mjemah, I.C. The Use of the DRASTIC-LU/LC model for assessing groundwater vulnerability to nitrate contamination in Morogoro Municipality, Tanzania. *Earth* **2022**, *3*, 1161–1184. [CrossRef]
34. Chakraborty, S.; Paul, P.K.; Sikdar, P.K. Assessing aquifer vulnerability to arsenic pollution using DRASTIC and GIS of North Bengal Plain: A case study of English Bazar Block, Malda District, West Bengal, India. *J. Spat. Hydrol.* **2007**, *7*, 101–121.
35. Saidi, S.; Bouri, S.; Ben Dhia, H. Sensitivity analysis in groundwater vulnerability assessment based on GIS in the Mahdia-Ksour Essaf aquifer, Tunisia: A validation study. *Hydrol. Sci. J.* **2011**, *56*, 288–304. [CrossRef]
36. Huan, H.; Wang, J.; Teng, Y. Assessment and validation of groundwater vulnerability to nitrate based on a modified DRASTIC model: A case study in Jilin City of northeast China. *Sci. Total Environ.* **2012**, *440*, 14–23. [CrossRef] [PubMed]
37. Tilahun, K.; Merkel, B.J. Estimation of groundwater recharge using a GIS-based distributed water balance model in Dire Dawa, Ethiopia. *Hydrogeol. J.* **2009**, *17*, 1443–1457. [CrossRef]
38. Kumar, A.; Pramod Krishna, A. Groundwater vulnerability and contamination risk assessment using GIS-based modified DRASTIC-LU model in hard rock aquifer system in India. *Geocarto Int.* **2020**, *35*, 1149–1178. [CrossRef]
39. Neshat, A.; Pradhan, B.; Pirasteh, S.; Shafri, H.Z.M. Estimating groundwater vulnerability to pollution using a modified DRASTIC model in the Kerman agricultural area, Iran. *Environ. Earth Sci.* **2014**, *71*, 3119–3131. [CrossRef]
40. Saranya, T.; Saravanan, S.; Jennifer, J.J.; Singh, L. Assessment of groundwater vulnerability in highly industrialized Noyyal basin using AHP-DRASTIC and Geographic Information System. In *Disaster Resilience and Sustainability*; Pal, I., Djalante, I., Shav, R., Shrestha, S., Eds.; Elsevier: Amsterdam, The Netherlands, 2007; pp. 151–170. [CrossRef]
41. Bera, A.; Mukhopadhyay, B.P.; Das, S. Groundwater vulnerability and contamination risk mapping of semi-arid Totko river basin, India using GIS-based DRASTIC model and AHP techniques. *Chemosphere* **2022**, *307*, 135831. [CrossRef]
42. Saranya, T.; Saravanan, S. Evolution of a hybrid approach for groundwater vulnerability assessment using hierarchical fuzzy-DRASTIC models in the Cuddalore Region, India. *Environ. Earth Sci.* **2021**, *80*, 1–25. [CrossRef]
43. Maretto, L.; Faccio, M.; Battini, D. A Multi-Criteria Decision-Making model based on fuzzy logic and AHP for the selection of digital technologies. *IFAC-PapersOnLine* **2022**, *55*, 319–324. [CrossRef]
44. Saranya, T.; Saravanan, S. Assessment of groundwater vulnerability using analytical hierarchy process and evidential belief function with DRASTIC parameters, Cuddalore, India. *Int. J. Environ. Sci. Technol.* **2023**, *20*, 1837–1856. [CrossRef]
45. Pacheco, F.; Pires, L.; Santos, R.; Sanches Fernandes, L. Factor weighting in DRASTIC modeling. *Sci. Total Environ.* **2015**, *505*, 474–486. [CrossRef]
46. Murgai, R.; Ali, M.; Byerlee, D. Productivity growth and sustainability in postgreen revolution agriculture: The case for the Indian and Pakistan Punjabs. *World Bank Res. Obser.* **2001**, *16*, 199–218. [CrossRef]
47. Gelberg, K.H.; Church, L.; Casey, G.; London, M.; Roerig, D.S.; Boyd, J.; Hill, M. Nitrate levels in drinking water in rural New York State. *Environ. Res.* **1999**, *80*, 34–40. [CrossRef]
48. TSMS (Turkish State Meteorological Service) MEVBİS. Available online: <https://mevbis.mgm.gov.tr/mevbis/ui/index.html> (accessed on 12 November 2022).

49. TUIK (Turkish Statistical Institute) Address Based Population Statistics of Turkey 2021. Available online: <https://data.tuik.gov.tr/Buletin/Index?p=Adrese-Dayali-Nufus-Kayit-Sistemi-Sonuclari-2021-45500> (accessed on 12 December 2022).
50. GDRS (General Directorate of Rural Services). *Soil Characteristics Map of Scale 1/25.000*; GDRS: Ankara, Turkey, 2001.
51. Güven, İ.H. *Doğu Karadeniz Bölgesi'nin 1/25.000 Ölçekli Jeolojisi ve Komplikasyonu*; MTA: Ankara, Turkey, 1993.
52. EEA (European Environment Agency). Copernicus Land Service—Pan-European Component: CORINE Land Cover 2000. European Environment Agency: Copenhagen. Available online: <https://land.copernicus.eu/pan-european/corine-land-cover/clc-2000?tab=download> (accessed on 2 December 2022).
53. EEA (European Environment Agency). Copernicus Land Service—Pan-European Component: CORINE Land Cover 2006. European Environment Agency: Copenhagen. Available online: <https://land.copernicus.eu/pan-european/corine-land-cover/clc-2006?tab=download> (accessed on 2 December 2022).
54. EEA (European Environment Agency). Copernicus Land Service—Pan-European Component: CORINE Land Cover 2012. European Environment Agency: Copenhagen. Available online: <https://land.copernicus.eu/pan-european/corine-land-cover/clc-2012?tab=download> (accessed on 2 December 2022).
55. EEA (European Environment Agency). Copernicus Land Service—Pan-European Component: CORINE Land Cover 2018. European Environment Agency: Copenhagen. Available online: <https://land.copernicus.eu/pan-european/corine-land-cover/clc2018?tab=download> (accessed on 2 December 2022).
56. Topuz, G.; Altherr, R.; Wolfgang, S.; Schwarz, W.H.; Zack, T.; Hasanözbe, A.; Mathias, B.; Satır, M.; Şen, C. Carboniferous high-potassium I-type granitoid magmatism in the Eastern Pontides: The Gümüşhane pluton (NE Turkey). *Lithos* **2010**, *116*, 92–110. [[CrossRef](#)]
57. Dokuz, A. A salt detachment and delamination model for the generation of Carboniferous high potassium I-type magmatism in the Eastern Pontides: The Köse composite Pluton. *Gondwana Res.* **2011**, *19*, 926–944. [[CrossRef](#)]
58. Yazıcı, N. Kelkit ve Köse (Gümüşhane) İlçe Merkezi İçme Sularının Hidrojeokimyasal Özellikleri İle Yan Kayaçlarla Olan İlişkilerinin İncelenmesi. Master's Thesis, Gümüşhane University Institute of Science, Gümüşhane, Turkey, 2019.
59. Robinson, A.G.; Banks, C.J.; Rutherford, M.M.; Hirst, J.P.P. Stratigraphic and structural development of the Eastern Pontides, Turkey. *J. Geol. Soc. Lond.* **1995**, *152*, 861–872. [[CrossRef](#)]
60. Şen, C. Jurassic volcanism in the Eastern Pontides: Is it rift related or subduction related? *Turk. J. Earth Sci.* **2007**, *16*, 523–539. Available online: <https://journals.tubitak.gov.tr/earth/vol16/iss4/6> (accessed on 16 November 2022).
61. Kandemir, R.; Yılmaz, C. Lithostratigraphy, facies and deposition environment of the Lower Jurassic Ammonitico Rosso Type Sediments (ARTS) in the Gümüşhane Area, NE Turkey: Implications for the opening of the Northern branch of the Neo-Tethys Ocean. *J. Asian Earth Sci.* **2009**, *34*, 586–598. [[CrossRef](#)]
62. Taslı, K. Gümüşhane-Bayburt Yörelerindeki Üst Jura-Alt Kretase Yaşı Karbonat İstiflerinin Stratigrafisi ve Mikropaleontolojik İncelemesi. Ph.D. Thesis, Karadeniz Technical University Graduate Institute of Natural and Applied Sciences, Trabzon, Turkey, 1990.
63. Yılmaz, C. Kelkit (Gümüşhane) yörenin stratigrafisi. *Jeoloji Mühendisliği* **1992**, *40*, 50–62. Available online: [https://www.jmo.org.tr/resimler/ekler/2a6845a557bef70\\_ek.pdf?dergi=JEOLOJ%DD%20M%DCHEND%DDSL%DD%D0%DD%20DERG%DDS%DD](https://www.jmo.org.tr/resimler/ekler/2a6845a557bef70_ek.pdf?dergi=JEOLOJ%DD%20M%DCHEND%DDSL%DD%D0%DD%20DERG%DDS%DD) (accessed on 16 November 2022).
64. Saydam Eker, Ç.; Sipahi, F.; Kaygusuz, A. Trace and rare earth elements as indicators of provenance and depositional environments of Lias Cherts in Gümüşhane NE Turkey. *Geochemistry* **2012**, *72*, 167–177. [[CrossRef](#)]
65. Arslan, M.; Aliyazıcıoğlu, I. Geochemical and Petrological Characteristics of the Kale (Gümüşhane) volcanic rocks: Implications for the Eocene evolution of Eastern Pontide arc volcanism, Northeast Turkey. *Int. Geol. Rev.* **2001**, *43*, 595–610. [[CrossRef](#)]
66. GDSHW (General Directorate of State Hydraulic Works)—Akım Gözlem Yıllıkları. Available online: <https://www.dsi.gov.tr/Sayfa/Detay/744#> (accessed on 14 December 2022).
67. Soysal, I.I. Assessment of groundwater vulnerability using modified DRASTIC-Analytical Hierarchy Process model in Bucak Basin, Turkey. *Arab. J. Geosci.* **2020**, *13*, 1127. [[CrossRef](#)]
68. Saaty, T.L. *The Analytic Hierarchy Process: Planning, Priority Setting, Resources Allocation*; McGraw: New York, NY, USA, 1980.
69. Karahan, M. Bulak (Kelkit, Gümüşhane) Göleti Aks Yeri ve Göl Alanındaki Kayaçların Geçirimlilik Özelliklerinin Araştırılması. Master's Thesis, Karadeniz Technical University Graduate Institute of Natural and Applied Sciences, Trabzon, Turkey, 2015.
70. Piscopo, G. Groundwater Vulnerability Map Explanatory Notes, Macquarie Catchment. NSW Department of Land and Water Conservation. Sydney, Australia, 2001. Available online: [https://www.dpie.nsw.gov.au/\\_data/assets/pdf\\_file/0010/151768/Macquarie-map-notes.pdf](https://www.dpie.nsw.gov.au/_data/assets/pdf_file/0010/151768/Macquarie-map-notes.pdf) (accessed on 1 December 2022).
71. Aydinalp, C.; Arslan, Y. Batı Karadeniz havzasındaki büyük toprak gruplarının FAO/UNESCO (1990), Fitzpatrick (1988) ve toprak taksonomisi (USDA soil taxonomy, 1994) sistemlerine göre sınıflandırılması. *ANADOLU Ege Tarımsal Araştırma Enstitüsü Derg.* **2003**, *13*, 188–200. Available online: <https://dergipark.org.tr/tr/pub/anadolu/issue/1774/21842> (accessed on 17 November 2022).
72. Tümsavaş, Z.; Aksoy, E. Kahverengi orman büyük toprak grubu topraklarının verimlilik durumlarının belirlenmesi. *J. Agric. Fac. Bursa Uludag Univ.* **2009**, *23*, 93–104. Available online: <https://dergipark.org.tr/tr/download/article-file/154090> (accessed on 17 November 2022).
73. Zeybek, İ. Turhal ovası ve yakın çevresi toprakları. *Türk Coğrafya Dergisi* **2003**, *41*, 41–61. Available online: <https://dergipark.org.tr/tr/download/article-file/198552> (accessed on 17 November 2022).

74. Singh, A.; Srivastav, S.K.; Kumar, S.; Chakrapani, G.J. A modified-DRASTIC model (DRASTICA) for assessment of groundwater vulnerability to pollution in an urbanized environment in Lucknow, India. *Environ. Earth Sci.* **2015**, *74*, 5475–5490. [[CrossRef](#)]
75. Bedient, P.B.; Rifai, H.S.; Newell, C.J. *Ground Water Contamination: Transport and Remediation*; Prentice Hall: Upper Saddle River, NJ, USA, 1999.
76. Spearman Rank Correlation Coefficient. In *The Concise Encyclopedia of Statistics*; Springer: New York, NY, USA, 2008; 502p. [[CrossRef](#)]
77. Napolitano, P.; Fabbri, A.G. Single-parameter sensitivity analysis for aquifer vulnerability assessment using DRASTIC and SINTACS. In *HydroGIS 96: Application of Geographical Information Systems in Hydrology and Water Resources Management, Proceedings of the Vienna Conference, Vienna, Austria, 16–19 April 1996*; IAHS Pub.: Wallingford, UK, 1996; Volume 235, pp. 559–566.
78. Boulding, J.R. *Practical Handbook of Soil, Vadose Zone, and Ground-Water Contamination: Assessment, Prevention, and Remediation*; CRC Press, Inc.: Boca Raton, FL, USA, 1995.
79. Saidi, S.; Bouri, S.; Dhia, H.B. Groundwater management based on GIS techniques, chemical indicators and vulnerability to seawater intrusion modelling: Application to the Mahdia-Ksour Essaf aquifer, Tunisia. *Environ. Earth Sci.* **2013**, *70*, 1551–1568. [[CrossRef](#)]
80. Zhang, Y.; Qin, H.; An, G.; Huang, T. Vulnerability assessment of farmland groundwater pollution around traditional industrial parks based on the improved DRASTIC Model—A case study in Shifang City, Sichuan Province, China. *Int. J. Environ. Res. Public Health* **2022**, *19*, 7600. [[CrossRef](#)] [[PubMed](#)]
81. Abera, K.A.; Gebreyohannes, T.; Abrha, B.; Hagos, M.; Berhane, G.; Hussien, A.; Belay, A.S.; Van Camp, M.; Walraevens, K. Vulnerability mapping of groundwater resources of Mekelle City and surroundings, Tigray Region, Ethiopia. *Water* **2022**, *14*, 2577. [[CrossRef](#)]
82. Jasrotia, A.S.; Singh, R. Groundwater pollution vulnerability using the DRASTIC model in a GIS environment, Devak-Rui Watersheds, India. *J. Environ. Hydrol.* **2005**, *13*, 11. Available online: <http://www.hydroweb.com/jeh/jeh2005/jasrotia.pdf> (accessed on 22 November 2022).
83. Brady, N.C.; Weil, R.R. *The Nature and Properties of Soils*; Prentice Hall: Englewood Cliffs, NJ, USA, 2002.
84. Chakraborty, B.; Roy, S.; Bera, A.; Adhikary, P.P.; Bera, B.; Sengupta, D.; Shit, P.K. Groundwater vulnerability assessment using GIS-based DRASTIC model in the upper catchment of Dwarakeshwar river basin, West Bengal, India. *Environ. Earth Sci.* **2022**, *81*, 1–15. [[CrossRef](#)]
85. Ersoy, A.F.; Gültekin, F. DRASTIC-based methodology for assessing groundwater vulnerability in the Gümüşhacıköy and Merzifon Basin (Amasya, Turkey). *Earth Sci. Res. J.* **2013**, *17*, 33–40.
86. Arafa, N.A.; Salem, Z.E.-S.; Ghorab, M.A.; Soliman, S.A.; Abdeldayem, A.L.; Moustafa, Y.M.; Ghazala, H.H. Evaluation of groundwater sensitivity to pollution using GIS-based modified DRASTIC-LU model for sustainable development in the Nile Delta Region. *Sustainability* **2022**, *14*, 14699. [[CrossRef](#)]
87. Secunda, S.; Collin, M.L.; Melloul, A.J. Groundwater vulnerability assessment using a composite model combining DRASTIC with extensive agricultural land use in Israel’s Sharon region. *J. Environ. Manag.* **1998**, *54*, 39–57. [[CrossRef](#)]
88. Huang, Y.; Zuo, R.; Li, J.; Wu, J.; Zhai, Y.; Teng, Y. The spatial and temporal variability of groundwater vulnerability and human health risk in the Limin District, Harbin, China. *Water* **2018**, *10*, 686. [[CrossRef](#)]
89. Sener, E.; Davraz, A. Assessment of groundwater vulnerability based on a modified DRASTIC model, GIS and an analytic hierarchy process (AHP) method: The case of Egirdir Lake basin (Isparta, Turkey). *Hydrogeol. J.* **2013**, *21*, 701–714. [[CrossRef](#)]
90. Hem, J.D. *Study and Interpretation of the Chemical Characteristics of Natural Water*; Water Supply Paper; U.S. Geological Survey: Washington, DC, USA, 1985; p. 2254.
91. Sharma, M.K.; Kumar, M. Sulphate contamination in groundwater and its remediation: An overview. *Environ. Monit. Assess.* **2020**, *192*, 74. [[CrossRef](#)]
92. Liu, J.; Han, G. Tracing riverine sulfate source in an agricultural watershed: Constraints from stable isotopes. *Environ. Pollut.* **2021**, *228*, 117740. [[CrossRef](#)]
93. Wang, H.; Zhang, Q. Research advances in identifying sulfate contamination sources of water environment by using stable isotopes. *Int. J. Environ. Res. Public Health* **2019**, *16*, 1914. [[CrossRef](#)]
94. Roy, A.; Keesari, T.; Mohokar, H.; Sinha, U.K.; Bitra, S. Assessment of groundwater quality in hard rock aquifer of central Telangana state for drinking and agriculture purposes. *Appl. Water Sci.* **2018**, *8*, 124. [[CrossRef](#)]
95. Javed, T.; Sarwar, T.; Ullah, I.; Ahmad, S.; Rashid, S. Evaluation of groundwater quality in district Karak Khyber Pakhtunkhwa, Pakistan. *Water Sci.* **2019**, *33*, 1–9. [[CrossRef](#)]
96. Lerner, D.N. Estimating Urban Loads of Nitrogen to Groundwater. *Water Environ. J.* **2003**, *17*, 239–244. [[CrossRef](#)]
97. Kurt, M.A.; Güler, C.; Alpaslan, M.; Akbulut, C. Determination of nitrate and nitrite origins in the soils and ground waters of the area between Mersin-Tarsus (Turkey) using geographic information systems. *Carpathian J. Earth Environ. Sci.* **2012**, *7*, 181–188.
98. Karadavut, İ.S.; Saydam, A.C.; Kalıpçı, E.; Karadavut, S.; Özdemir, C. A research for water pollution of Melendiz stream in terms of sustainability of ecological balance. *Carpathian J. Earth Environ. Sci.* **2011**, *6*, 65–80.
99. Prasanth, S.S.; Magesh, N.; Jitheshlal, K.; Chandrasekar, N.; Gangadhar, K. Evaluation of groundwater quality and its suitability for drinking and agricultural use in the coastal stretch of Alappuzha District, Kerala, India. *Appl. Water Sci.* **2012**, *2*, 165–175. [[CrossRef](#)]

100. Saravanan, S.; Pitchaikani, S.; Thambiraja, M.; Sathiyamurthi, S.; Sivakumar, V.; Velusamy, S.; Shanmugamoorthy, M. Comparative assessment of groundwater vulnerability using GIS-based DRASTIC and DRASTIC-AHP for Thoothukudi District, Tamil Nadu India. *Environ. Monit. Assess.* **2023**, *195*, 57. [[CrossRef](#)]
101. Awais, M.; Aslam, B.; Maqsoom, A.; Khalil, U.; Ullah, F.; Azam, S.; Imran, M. Assessing Nitrate Contamination Risks in Groundwater: A Machine Learning Approach. *Appl. Sci.* **2021**, *11*, 10034. [[CrossRef](#)]
102. Jahromi, M.N.; Gomeh, Z.; Busico, G.; Barzegar, R.; Samany, N.N.; Aalami, M.T.; Tedesco, D.; Mastrocicco, M.; Kazakis, N. Developing a SINTACS-based method to map groundwater multi-pollutant vulnerability using evolutionary algorithms. *Environ. Sci. Pollut. Res.* **2021**, *28*, 7854–7869. [[CrossRef](#)] [[PubMed](#)]
103. Dhaoui, O.; Antunes, I.; Agoubi, B.; Kharroubi, A. Integration of water contamination indicators and vulnerability indices on groundwater management in Menzel Habib area, south-eastern Tunisia. *Environ. Res.* **2022**, *205*, 112491. [[CrossRef](#)]
104. Hasan, M.; Islam, M.A.; Aziz Hasan, M.; Alam, M.J.; Peas, M.H. Groundwater vulnerability assessment in Savar upazila of Dhaka district, Bangladesh—A GIS-based DRASTIC modeling. *Groundw. Sustain. Dev.* **2019**, *9*, 100220. [[CrossRef](#)]
105. Salek, M.; Levison, J.; Parker, B.; Gharabaghi, B. CAD-DRASTIC: Chloride application density combined with DRASTIC for assessing groundwater vulnerability to road salt application. *Hydrogeol. J.* **2018**, *26*, 2379–2393. [[CrossRef](#)]
106. Moratalla, Á.; Gómez-Alday, J.J.; Sanz, D.; Castaño, S.; De Las Heras, J. Evaluation of a GIS-based integrated vulnerability risk assessment for the Mancha Oriental System (SE Spain). *Water Resour. Manag.* **2011**, *25*, 3677–3697. [[CrossRef](#)]
107. Sakala, E.; Fourie, F.; Gomo, M.; Coetzee, H. GIS-based groundwater vulnerability modelling: A case study of the Witbank, Ermelo and Highveld Coalfields in South Africa. *J. Afr. Earth Sci.* **2018**, *137*, 46–60. [[CrossRef](#)]
108. Jamrah, A.; Al-Futaisi, A.; Rajmohan, N.; Al-Yaroubi, S. Assessment of groundwater vulnerability in the coastal region of Oman using DRASTIC index method in GIS environment. *Environ. Monit. Assess.* **2008**, *147*, 125–138. [[CrossRef](#)] [[PubMed](#)]
109. Haidu, I.; Nistor, M. Groundwater vulnerability assessment in the Grand Est region, France. *Quat. Int.* **2020**, *547*, 86–100. [[CrossRef](#)]

**Disclaimer/Publisher’s Note:** The statements, opinions and data contained in all publications are solely those of the individual author(s) and contributor(s) and not of MDPI and/or the editor(s). MDPI and/or the editor(s) disclaim responsibility for any injury to people or property resulting from any ideas, methods, instructions or products referred to in the content.